12-1982

Kinetics of Ternary Complex Formation Reactions of the Nickel(II) Complexes of Ethylenediaminediacetate and Triethylenetetramine with Bidentate Donors

Lawrence H. Kolopajlo
Western Michigan University

KINETICS OF TERNARY COMPLEX FORMATION. REACTIONS OF THE NICKEL(II) COMPLEXES OF ETHYLENEDIAMINE-DIACETATE AND TRIETHYLENETETRAMINE WITH BIDENTATE DONORS

by

Lawrence H. Kolopajlo

A Dissertation
Submitted to the
Faculty of The Graduate College
in partial fulfillment of the
requirements for the
Degree of Doctor of Philosophy
Department of Chemistry

Western Michigan University
Kalamazoo, Michigan
December 1982

KINETICS OF TERNARY COMPLEX FORMATION.
REACTIONS OF THE NICKEL(II) COMPLEXES OF ETHYLENEDIAMINE-DIACETATE AND TRIETHYLENETETRAMINE WITH BIDENTATE DONORS

Lawrence H. Kolopajlo, Ph.D.

Western Michigan University, 1982

The stopped-flow technique was used to measure rate constants for ternary complex formation involving both NiEDDA and $Ni(trien)^{2+}$, and bidentate donors. The reactions of both NiEDDA and $Ni(trien)^{2+}$ with bipy, phen, en, and sar were studied. In addition the reaction of NiEDDA and gly was studied. The reactions were of the first-order with respect to either nickel complex, and with respect to enH^+, bipy, and phen. The reactions involving phen and bipy were independent of pH and were reversible. The formation rate constants for the systems containing diamine reactants are as follows:

$k_{NiE}^{phen} = 4.3 \times 10^3\ M^{-1}s^{-1}$, $k_{NiE}^{bipy} = 5.5 \times 10^3\ M^{-1}s^{-1}$,

$k_{NiE}^{enH^+} = 1.0 \times 10^3\ M^{-1}s^{-1}$, $k_{NiT}^{phen} = 8.2 \times 10^3\ M^{-1}s^{-1}$,

$k_{NiT}^{bipy} = 7.6 \times 10^3\ M^{-1}s^{-1}$, and $k_{NiT}^{enH^+} = 1.3 \times 10^3\ M^{-1}s^{-1}$. For systems reactions are: k_b(NiE-bipy) $= 8.0 \times 10^{-2}\ s^{-1}$, k_b(NiE-phen) $= 3.0\ s^{-1}$, k_b(NiT-bipy) $= 0.18\ s^{-1}$, and k_b(NiT-phen) $= 5.3\ s^{-1}$. The reactions

reactions are: k_b(NiE-bipy) $= 8.0 \times 10^{-2}\ s^{-1}$, k_b(NiE-phen) $= 3.0\ s^{-1}$, k_b(NiT-bipy) $= 0.18\ s^{-1}$, and k_b(NiT-phen) $= 5.3\ s^{-1}$. The reactions of NiEDDA with phen and bipy proceeded at a normal rate. In contrast, the formation rate constants for the reactions of bipy and phen with $Ni(trien)^{2+}$ were lower than expected by factors of 36 and 33 respectively. Also, stability constants for $(trien)Ni(phen)^{2+}$,

and (trien)Ni(bipy)$^{2+}$ were lower than expected. For these latter reactions, the reduced formation rates and stabilities are attributed to steric hindrance on the part of trien. The reactions of gly and sar with NiEDDA, and of sar with Ni(trien)$^{2+}$ were of the first-order with respect to amino acid at low concentration, and shifted to a zero-order dependence with respect to gly or sar at high amino acid concentration. A two step mechanism was supported from the kinetics. The first step involves an oxygen bonded intermediate in rapid equilibrium with reactants. The equilibrium constants for this step are: K_1(NiE-gly) = 1.9 x 10^2 M^{-1}, K_1(NiE-sar) = 93 M^{-1}, and K_1(NiT-sar) = 430 M^{-1}. The second step, which is rate limiting, involves a slow ring closure; the corresponding rate constants are: k_2(NiE-gly) = 44 s^{-1}, k_2(NiE-sar) = 44 s^{-1}, and k_2(NiT-sar) = 68 s^{-1}. The results show that (1) steric hindrance imposed by a tetradentate ligand coordinated to nickel(II), as well as (2) the type of donor sites on the attacking bidentate ligand, can greatly alter the mechanism of ternary complex formation.

Kolopajlo, Lawrence Hugh

KINETICS OF TERNARY COMPLEX FORMATION. REACTIONS OF THE NICKEL(II) COMPLEXES OF ETHYLENEDIAMINEDIACETATE AND TRIETHYLENETETRAMINE WITH BIDENTATE DONORS

Western Michigan University PH.D. 1982

ACKNOWLEDGEMENTS

To Professor Ralph K. Steinhaus, my research advisor, I wish to express my sincere appreciation for his expert guidance and support during the completion of this work.

I also appreciate the generosity of Dr. Robert H. Anderson who advised me on computer calculations. In addition, I appreciate the interesting suggestions and discussions with Dr. George Lowry, Dr. Dean Cooke, and also Dr. Michitoshi Soga of the Physics Department.

To my wife Mary, and to my parents as well as hers, I am especially indebted for their kindness and encouragement.

I also gratefully acknowledge the partial support received from the Graduate College of Western Michigan University.

Lawrence H. Kolopajlo

TABLE OF CONTENTS

Table of Contents (Continued)

LIST OF TABLES

List of Tables (Continued)

LIST OF FIGURES

List of Figures (Continued)

CHAPTER I

INTRODUCTION

Investigations into the mechanistic nature of complex formation reactions in water have received a substantial amount of attention[1]. Empirical studies[2] have been carried out using a variety of fast reaction techniques including stopped-flow, temperature-jump, pressure-jump, sound absorption, and NMR line broadening. As a further step towards the elucidation of the kinetics and mechanisms of ternary complex formation, the present study has used the stopped-flow method to define the reactions of both NiEDDA (N,N'-ethylenediaminediacetatonickel(II)) and $Ni(trien)^{2+}$ (triethylenetetraminenickel(II)) with a series of bidentate donors.

The general mechanism[3] proposed by Eigen and Tamm has been successful in predicting experimentally determined rate constants for many 1:1 complex formation reactions involving a variety of ligands. For the reaction of aquated Ni^{2+} with a bidentate ligand, the Eigen-Tamm mechanism is written as follows:

$$Ni(H_2O)_6^{2+} + (L\text{-}L)^{n-} \underset{}{\overset{K_{os}}{\rightleftharpoons}} \underset{A}{Ni(H_2O)_6 \cdot (L\text{-}L)^{2-n}} \qquad (1)$$

$$A \underset{k\text{-}1}{\overset{k_1}{\rightleftharpoons}} \underset{B}{(H_2O)_5Ni\text{-}L\text{-}L^{\,2-n}} + H_2O \qquad (2)$$

$$B \underset{k\text{-}2}{\overset{k_2}{\rightleftharpoons}} \underset{C}{(H_2O)_4Ni\begin{smallmatrix}L\\|\\L\end{smallmatrix}^{\,2-n}} + H_2O \qquad (3)$$

In the above reaction sequence, $(L\text{-}L)^{n-}$ represents the bidentate reactant whereas $Ni(H_2O)_6^{2+}$ is the aquated nickel ion in solution. The initial step (1) represents a diffusion controlled rapid pre-equilibrium of reactants to form an outer-sphere complex A whose association constant K_{os} is calculated according to the theoretical expression:

$$K_{os} = \frac{4\pi Na^3}{3000} \exp(-U/kT) \qquad (4)$$

A definition of the symbols used in equation (4) is given in Chapter Four (page 73). In the second step of the Eigen-Tamm model, species A loses a water molecule from the inner coordination sphere of the nickel ion, and this process is immediately followed by coordination of the ligand L-L to give the monocoordinated species B. The forward rate constant for step (2) is denoted

$$k_1 = k^{Ni\text{-}H_2O} \qquad (5)$$

This latter equation describes water exchange at nickel. The reverse process in (2) involves rupture of the Ni-L bond to form A, and the corresponding reverse rate constant is called k_{-1}. The final step (3) describes the loss of a second coordinated water molecule from the inner coordination sphere of species B, followed by ring closure of L-L to form the binary complex, species C. The forward and reverse rate constants for the last step are given by k_2 and k_{-2} respectively.

In order to derive a rate expression for product formation using the Eigen-Tamm mechanism, three assumptions are normally made:

(a) the pre-equilibrium (1) is rapid

(b) the monocoordinated species B is a steady state intermediate

(c) k_{-2} is small and may be neglected

Using these three assumptions, the derived rate law for product formation is written

$$\frac{d[C]}{dt} = \frac{K_{os}k_1k_2}{(k_{-1} + k_2)} \left[Ni(H_2O)_6^{2+}\right]\left[(L_2)^{n-}\right] \qquad (6)$$

Thus the kinetic behavior is expected to be of the first-order with respect to each reactant, with an overall second-order rate constant k_f given by

$$k_f = \frac{K_{os}k_1k_2}{(k_{-1} + k_2)} \qquad (7)$$

Much empirical evidence has accumulated to indicate that the rate limiting step of the Eigen-Tamm mechanism often involves water loss from species A. If this is the case, then ring closure, step (3) is fast so that $k_2 \gg k_{-1}$. Under this condition, the reaction velocity is said to be normal, and equation (7) simplifies to

$$k_f = k_1K_{os} = k^{Ni-H_2O}\,K_{os} \qquad (8)$$

so that the rate coefficient k_f can be predicted from calculated values of K_{os} and independent measurements of k^{Ni-H_2O}.

The Eigen-Tamm equation, as given in (8), is readily derived, easily understood, and has consistently provided effective descriptions of the rate behavior for systems involving metal ions and monodentate ligands. Consequently, it has been widely used to interpret kinetic data pertaining to many types of complex formation

reactions. However, equation (8) does not provide a satisfactory representation of much of the kinetic data. Significant deviations from projected k_f values given by Eq. (8) have been identified. For example, it has been found that the rate behavior of complex formation reactions sometimes depends on both the physical and chemical natures of the reacting species. Electrostatic, steric, and basicity effects are just a few of the factors that can complicate the interpretation of rate behavior based on Eq. (8). These complications can even cause a shift in the location of the rate determining step, for example, from initial coordination to ring closure.

Although the kinetics and mechanisms of binary complex formation reactions have received much attention, comparatively little has been reported on the analogous ternary complex formation reactions. In the context of the present study, a ternary complex is defined as a complex composed of two different ligands coordinated to a metal ion. The corresponding chemical reaction for the ligands L and L' is

$$ML + L' \longrightarrow MLL' \qquad (9)$$

Investigations into the nature of the formation of ternary complexes are important because these complexes play a part in the catalytic reactions of biochemical systems[4]. In addition, fundamental problems in chemical kinetics are involved.

Most of the reported studies[5] concerning the formation of mixed ligand complexes have centered on the reactions between attacking ligands L' that are monodentate and Ni(II) complexes that contain

bi- or tri-dentate ligands. These studies have shown that vacant coordination sites on the metal complex are not sterically hindered. A few studies have been reported on the reactions of monodentate ligands with tetradentate Ni(II) complexes[5]. Even fewer investigations have been launched to identify the steric considerations affecting the reaction between a bidentate ligand and a tetradentate Ni(II) complex. Reactions involving nickel(II) are often studied because, compared to the other bivalent metal ions, they are less reactive so that fewer experimental problems are involved. Therefore the study of potentially sterically hindered formation reactions between tetradentate Ni(II) complexes and bidentate reactants was believed to provide a good dissertation topic.

The Eigen-Tamm model, as described in equations (1)-(3) for binary complex formation, is easily extended to ternary complex formation. Deviations of experimental values from predicted ones then indicate steric or mechanistic effects of the coordinated ligand on the formation rate.

One general rule[6] that has emerged from studies on ternary complex formation is that both k_f and k^{Ni-H_2O} increase as the number of aliphatic nitrogens coordinated to nickel is increased. Thus the reaction between $Ni(NTA)^-$ and NH_3 was found to be slower than the one between $Ni(trien)^{2+}$ and NH_3 (by a factor of 71) since trien contains four coordinated N atoms and NTA^{3-} only contains one[7]. When this empirical rule was taken into consideration, certain systems which at first did not appear to show predictable kinetic behavior were

then rationalized in terms of Eq. (8). This was done by using corrected values for the rates of water loss, which take into account the accelerating effects of coordinated N atoms. Another set[8] of studies involved the reactions of NSA^-, a bidentate ligand, with a series of Ni(II) complexes whose coordinated ligands were: NTA^{3-}, $EDDA^{2-}$, dien, trien, and tren. In Table 1 and Figure 1 are listed the names and structures of these and other ligands referred to in this study. These latter mentioned complexes contain one, two, three, and four N atoms respectively. A pronounced trend was shown by these complexes which are tetradentates (except for dien which is a tridentate). It was found that NTA^{3-} was the least reactive of the coordinated ligands while trien and tren were the most reactive compared to NTA^{3-}, by factors of 318 and 364 respectively. The coordinated ligand $EDDA^{2-}$ was about twice as reactive as NTA^{3-} while dien was 70 times higher in reactivity. A third set of studies[9] examined the reactions of the bidentate ligand PADA with several of the above mentioned nickel(II) complexes. Except for trien and tren, when the influence of the varying numbers of N donor atoms, and the charge on both the ligand and metal ion was considered, the observed rate behavior could be described by Eq. (8). However, in the case of trien and tren, the differences between predicted and observed rate constants were attributed to ring closure contributing to the rate limiting step. An example of this latter effect was reportedly[9] shown from a comparison of the formation rate constants for reactions (10) and (11):

$$Ni(NTA)^- + NH_3 \longrightarrow (NH_3)Ni(NTA)^- \qquad (10)$$

TABLE 1

List of Abbreviations and Symbols

bipy	2,2'-bipyridine
dien	diethylenetriamine
EDDA;E	N,N'-ethylenediaminediacetic acid
EDTA	ethylenediaminetetraacetic acid
en	ethylenediamine
gly	glycine
gly^-	glycinate
HEPES	N-2-hydroxyethlypiperazine-N'-2-ethanesulfonic acid
NSA^-	5-nitrosalicylate
NTA^{3-}	nitrilotriacetate
OAc^-	acetate
PADA	pyridine-2-azo-p-dimethylaniline
phen	1,10-phenanthroline
py	pyridine
pya_2tn	N,N'-bis(2-pyridylmethylene)-1,3-diaminopropane
sar	sarcosine, N-methylglycine
sar^-	N-methylglycinate
TAPS	tris[hydroxymethyl] methylaminopropane sulfonic acid
tren	2,2',2''triaminotriethylamine
trien;T	triethylenetetramine
ICB	internal conjugate base

Table 1 (continued)

I	ionic strength
λ	wavelength
t	time

en $H_2N-CH_2-CH_2-NH_2$

gly H_2N-CH_2-COOH

sar

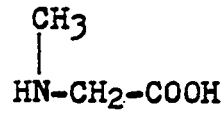

EDDA

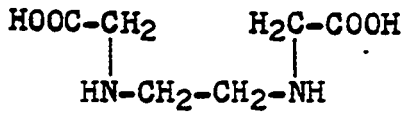

dien

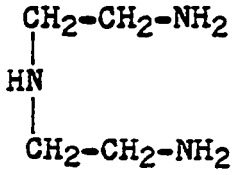

tren

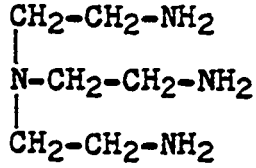

FIGURE 1. Structures of Some Multidentate Ligands

trien

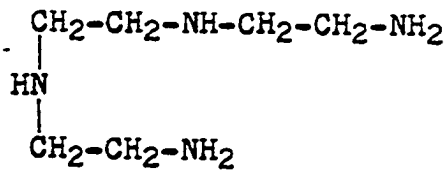

NTA

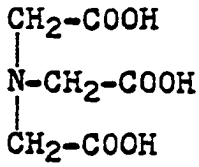

NSA

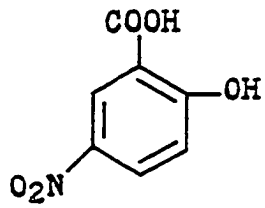

bipy

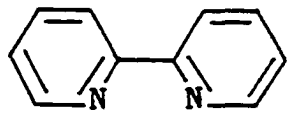

phen

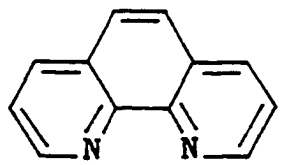

PADA

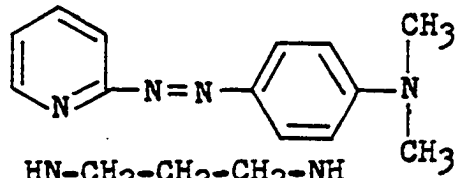

pya_2tn

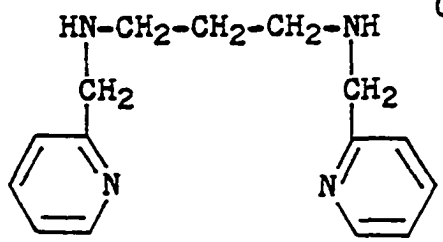

FIGURE 1 (continued)

$$Ni(trien)^{2+} + PADA \longrightarrow (PADA)Ni(trien)^{2+} \qquad (11)$$

The experimental results showed that reaction (11) was six times faster than reaction (10). However, on the basis of reported results for the addition of NH_3 to both $Ni(NTA)^-$ and $Ni(trien)^{2+}$, the ratio of formation rate constants (11)/(10) should be about 40. The difference between expected and observed rate constants was, as stated above, rationalized in terms of a ring closure contribution to the rate limiting step of the $Ni(trien)^{2+}$-PADA reaction. The slow ring closure was believed to be a result of a steric hindrance effect from the coordinated trien. Mechanistically a three step process, similar to that shown in equations (1) to (3) is required for the $Ni(trien)^{2+}$-PADA reaction, whereas for the $Ni(trien)^{2+}$-NH_3 reaction, the third step is absent.

Wilkins[10] reported on the reactions of $Ni(tren)^{2+}$ with 1,10-phenanthroline, 2,2'-bipyridine, and glycine. The results showed that ring closure played a role in the rate limiting step of each of the above reactions.

Another report[11] concerned the reactions of $Ni(pya_2tn)$ with NH_3, ethylamine, glycine, and alanine. The observed formation constant k_f could not be compared to a predicted value from equation (8), however, because rate of water loss data is not available for $Ni(pya_2tn)$. It was also found that ethylamine reacted five times slower than ammonia, and the conclusion was that the bound tetra-chelated ligand pya_2tn hindered ethylamine more than NH_3. The corresponding reactions for both glycine and alanine were markedly slower than those for either ammonia or ethylamine. This result

was interpreted as being due to a rearrangement of pya_2tn on nickel- from square planar geometry to cis-octahedral geometry, as required to accommodate the bidentate ligands.

Steinhaus and Lee[12] recently reported on the reactions of $Ni(trien)^{2+}$ with both phen and glycine. For the $Ni(trien)^{2+}$-phen system, the formation rate constant turned out to be lower than predicted using Eq. (8), by a factor of 35. These results were interpreted according to the Eigen-Tamm model, with a steric hindrance imposed by trien. The kinetic behavior for the $Ni(trien)^{2+}$-glycine reaction revealed a nonlinear dependence between the rate constant and the glycinate ion concentration. This dependence was accompanied by a change in reaction order with respect to glycine concentration from first to zero. The mechanistic interpretation involved the formation of an intermediate (having weakly coordinating oxygen bonded to nickel) in rapid equilibrium with reactants, followed by a sluggish ring closure. This latter process becomes rate limiting at high glycine concentrations.

As stated previously, the present study is concerned with the kinetics and mechanisms of ternary complex formation involving tetradentate Ni(II) complexes and a series of bidentate ligands. The first set of kinetic studies were initiated on the reactions of $Ni(trien)^{2+}$, a sterically hindered complex, with ethylenediamine, bipyridine, phenanthroline, and sarcosine. The second part of this study centers on the reactions of NiEDDA, a complex with different steric requirements than $Ni(trien)^{2+}$, and with a much lower rate of water loss. In order to make possible a comparison of the reactions

of NiEDDA with those of $Ni(trien)^{2+}$, the following bidentate donors were chosen for study: ethylenediamine, bipyridine, phenanthroline, glycine, and sarcosine.

CHAPTER II

EXPERIMENTAL

Chemicals

Reagent grade chemicals were used except as noted. All solutions were made using deionized water which was prepared by passing distilled water through an ion exchange column containing a mixed bed resin (Amberlite MB-3).

Acetic acid-sodium acetate buffer

Sodium acetate ($NaC_2H_3O_2 \cdot 3H_2O$) from J. T. Baker Co. (270 g) was dissolved along with 60 ml of glacial acetic acid to give one liter of water to give a 3 M solution (acetate concentration) at pH 5.

Boric acid-sodium borate buffer

Borate buffer at pH 9 was prepared by mixing equal amounts of 0.1 M solutions of sodium tetraborate ($Na_2B_4O_7 \cdot 10H_2O$) and boric acid (H_3BO_3). The pH of this buffer system could be adjusted by addition of mannitol.

HEPES Buffer

The buffer HEPES (N-2-hydroxyethylpiperazine-N'-2-ethanesulfonic acid) was obtained from SIGMA Chemical Co. This buffer was used over the 6.8 to 8.2 pH range in the concentration range 0.02 to 0.1 M.

TAPS buffer

The buffer TAPS (tris [hydroxymethyl] methylaminopropane sulfonic acid) was also obtained from SIGMA Chemical Co. TAPS was used over the pH range 7.7 to 9.1 at concentrations from 0.01- to 0.125-M.

Primary standard copper nitrate

A standard solution of copper nitrate was prepared by weight from heavy copper foil. This latter constituent at 99.96% purity was obtained from J. T. Baker Co. The preparation entailed rinsing the foil with dilute nitric acid, deionized water, and absolute ethanol. The copper foil was then dried, weighed, and dissolved in a minimum amount of concentrated nitric acid. After dilution to volume, the concentration was 0.09994 M.

Nickel(II) nitrate

Nickel(II) nitrate was obtained from J. T. Baker Co. as the hexahydrate. A solution was prepared and standardized at pH 5.5 by titration with EDTA using murexide as indicator.

2,2'-Bipyridine

2,2'-Bipyridine (melting point 70-71°C) was supplied from Matheson Coleman & Bell. This compound was used without further purification. A solution (0.0150 M) was prepared by weight.

1,10-Phenanthroline

1,10-Phenanthroline (G. Frederick Smith Chemical Co.) was used without additional purification. A solution at 0.150 M was prepared by weight, the concentration being near the maximum solubility of phen in water.

Ethylenediamine

The above compound at 99% purity was obtained from the Aldrich Chemical Co. and further purification was carried out. The process involved digesting a 350 ml sample over 40 grams of NaOH pellets on a steam bath overnight. A $CaCl_2$ drying tube was employed to protect the system from atmospheric moisture. Distillation was performed at 166°C, and the middle fraction boiling at this temperature was retained. A solution of en at an approximate concentration of 0.5 M was prepared by volume. Standardization was performed by a potentiometric titration against standard HCl. The final concentration of the en solution was 0.491 M.

Glycine

Aldrich glycine (98% pure) was purified by two recrystallizations from a water-methanol solution which was 1% methanol by volume.

Sarcosine

N-methylglycine (98% pure) was obtained from the Aldrich

Chemical Company. It was recrystallized from a methanol-water solution, which was 7% H_2O volume.

EDTA

Ethylenediaminetetraacetic acid, disodium salt dihydrate, was supplied by the Aldrich Chemical Company. The purity of this compound was in excess of 99% (Gold Label brand). Standardization of EDTA was performed by a titration against standard copper nitrate solution at pH 10, using murexide as indicator.

Ethylenediaminediacetic acid

Reagent grade EDDA (SIGMA Chemical Co.) was purified by two recrystallizations from a hot basic solution, by addition of perchloric acid. After drying, the melting point was at 209-210°C. The mole ratio method was used to standardize the EDDA with standard $Cu(NO_3)_2$ at a wavelength of 670 nm and pH 5 (acetic acid-sodium acetate buffer).

Triethylenetetramine

Reagent grade triethylenetetramine disulfate ($C_6H_{18}N_4 \cdot 2H_2SO_4$) from J. T. Baker Co. was twice recrystallized by the addition of methanol to a hot aqueous solution. The compound was filtered and washed with cold methanol. A tenth molar solution was prepared and standardized using the mole ratio method, against $Ni(NO_3)_2$ at 567 nm. The buffer system employed was ammonia-ammonium chloride at pH 10.

(Triethylenetetramine)nickel(II)

In order to prepare a $Ni(trien)^{2+}$ solution, a slight molar excess (about 5%) of nickel(II) nitrate solution was added to a trien solution. The pH was adjusted to 11, to precipitate the excess nickel as the hydroxide. The solution was then filtered through a 0.45 micron Millipore filter, in order to remove the precipitate of Ni(II) hydroxide. The resulting solution was clear, and its pH was lowered to 9 by the addition of sulfuric acid. A spectrophotometric method was employed to standardize the $Ni(trien)^{2+}$ solution. The standardization involved determination of the nickel content at 267 nm. This was accomplished by adding a 100-fold excess of KCN (using the ammonia-ammonium chloride buffer system at pH 10) to the unknown to obtain $Ni(CN)_4^{2-}$. The absorbance of this latter solution was then compared to the absorbance of a standard tetracyanonickelate(II) solution prepared from standard $Ni(NO_3)_2$ and a 100-fold excess of KCN at pH 10.

(Ethylenediamine-N,N'-diacetate)nickel(II)

The complex NiEDDA was prepared and standardized in the same manner as described above for $Ni(trien)^{2+}$.

Apparatus and Procedure

All spectra were recorded using a Cary Model 14 spectrophotometer. The kinetic measurements were made using an Aminco Morrow Stopped-Flow Apparatus attached to a Shimadzu QV-50 spectrophotometer.

A Tektronix 5103N storage oscilloscope was employed to monitor the spectral changes. In addition, these spectral changes were stored on a Biomation Waveform Recorder (Model 805) and displayed from memory on a Model SR Sargent Recorder.

A Beckman Research Model pH Meter, which possesses a relative accuracy of $\pm$ 0.001 pH unit, was employed for pH measurements. The final pH for each solution was obtained by measuring the pH of a solution produced by mixing equal amounts of reactants, which had been adjusted to the desired pH. The values of pH for the mixed solutions agreed with those set for each reactant before mixing. Several buffers were employed to maintain the desired pH. HEPES buffer (N-2-hydroxyethylpiperazine-N'-2-ethanesulfonic acid) was used over the pH range 6.8 to 8.2. TAPS buffer (tris[hydroxymethyl]-methylaminopropane sulfonic acid) was used over the pH range 7.7-9.1. The pK_a values for HEPES and TAPS are 7.5 and 8.4 respectively at 25°C. HEPES and TAPS were used in all except a few kinetic runs which were performed using a boric acid-sodium borate buffer system at pH values of 7.5, 8.0, and 8.1. These latter runs were made on the NiEDDA-bipy reaction system.

The formation of mixed ligand complexes was examined using a stopped-flow technique. Prior to each run, the pH of each reactant was adjusted to the desired value. The ionic strength, I, was adjusted to 0.1 M using 1.0 M NaCl solution. The temperature was maintained at 25.0±0.1°C by means of a constant temperature bath connected to the reservoir site of a compartment within the stopped-flow apparatus. The wavelength control of the Schimadzu QV-50

spectrophotometer was set at a value which gave a maximum absorbance change between product and reactant. In this procedure, absorption spectra of aqueous solutions of the ligand L, the nickel(II) complex NiL, and the ternary complex NiLL' were taken at known concentrations of their respective solutions. These spectra were taken in the ultraviolet spectral region in which the ligand L showed a weak absorption. However, the absorptions of the complexes NiL and NiLL' were much stronger. It was possible to find a wavelength at which there was a marked difference between the absorptions of these latter two complexes, and this wavelength was chosen to monitor the kinetics of reactions between NiL and L'. Some of the absorption spectra were reported by Lee[13] while others were determined in the present study. The reactions of $Ni(trien)^{2+}$ and a number of ligands were followed directly: phen(343 nm), bipy(305 nm), en(252 nm), and sar(242 nm). The reactions of NiEDDA with a number of bidentate donors were also directly monitored: phen(343 nm), bipy(305 nm), en(254 nm), gly(240 nm), and sar(242 nm).

In each reactant system the formation of ternary complex was followed by measurement of percent transmittance (% T) versus time t. A preliminary run was performed in order to obtain a value for the final percent transmittance which could be read from the oscilloscope trace. On initiating a reaction, % T values versus time changes were stored in the Biomation Waveform Recorder as the reaction progressed. These values were subsequently displayed on a Sargent Model S R Recorder. From this latter trace, it was possible to make a table of % T vs. time, which was then entered into a computer file so that

calculations, for the purpose of extracting rate coefficients from the data, could be performed. For each system, the concentration of the ligand reactant or the pH was systematically varied over a wide range. Thus each reported kinetic run is for a specific set of reaction conditions, and also, each reported kinetic run is the average of from three to six separate stopped-flow runs.

CHAPTER III

RESULTS

Data Reduction

All reactions were carried out to completion. Biphasic behavior was not observed in either the stopped-flow trace or in the subsequent data reduction as illustrated by the linear behavior of the appropriate kinetic plots, which described a specific function of the rate constant for the reaction system involved. For all runs, pseudo-first-order conditions were maintained by using at least a ten-fold excess (in total concentration) of ligand reactant with respect to nickel(II) chelate concentration.

For the treatment of the data provided by the rate studies, a computer calculation was involved. More specifically a computer program was utilized for the purpose of effecting data reduction and error analysis. The method used involved a non-linear least squares analysis. The input data set for this program consisted of percent transmittance versus time values for a completed kinetic run. The output data set calculated from the input data set consisted of three parameters and their corresponding standard deviations. Two of the output variables, A_f and Al, were absorbance values. The first of these output variables, A_f, represents the final absorbance value for the reaction; this corresponds to time infinity. The latter

output variable Al represents the absorbance change of the reaction, denoted by $A_f - A_i$, where A_i is the initial absorbance of the reaction mixture. In the present studies, the formation of ternary complex was followed, so that absorbance values always increased with reaction time t. The third and most important parameter obtained from the computer calculation was k^o, the pseudo-first-order rate constant. The formula in which all three of the above output variables are expressed is given by:

$$A_t = (A_i - A_f)\exp(-k^o t) + A_f \qquad (12)$$

On the left-hand side of the above equation, the term A_t is the absorbance of the product mixture at time t. Rate constants for all kinetic runs were obtained by applying the method described above. However, for purposes of comparison, on a few runs a conventional least-squares treatment was applied to the integrated formula for a pseudo-first-order reaction. The resulting kinetic plots showed good first-order behavior. In the following sections, each reported rate constant k^o is the average of at least three individual runs at the same set of conditions. Table 2 lists the ranges of ligand concentration and pH that were used in the present study for each reaction system.

Kinetic Systems Involving NiEDDA

NiEDDA-En Reaction

The above system was followed over the pH range 6.8 to 8.5 using both HEPES and TAPS buffers at a concentration of 0.1 M.

TABLE 2

Concentration and pH Conditions Used for Reaction Rate Studies[a]

Reaction System	Concentration Range of Ligand[b] M	pH
NiEDDA-bipy	1.5×10^{-4} to 1.7×10^{-3}	7.5, 8.0, 8.1
NiEDDA-phen	1.8×10^{-4} to 6.0×10^{-3}	7.4, 8.0, 8.5
NiEDDA-en	constant at 0.025	6.8 to 8.5
NiEDDA-gly	0.013 to 0.10	6.8 to 9.1
NiEDDA-sar	0.013 to 0.11	6.8 to 9.1
$Ni(trien)^{2+}$-bipy	1.8×10^{-4} to 2.0×10^{-3}	7.4, 8.0
$Ni(trien)^{2+}$-phen	2.1×10^{-4} to 5.98×10^{-3}	7.1, 7.5, 8.0
$Ni(trien)^{2+}$-en	constant at 0.059	6.9 to 8.8
$Ni(trien)^{2+}$-sar	0.013 to 0.10	6.9 to 8.8

a. Ionic strength, I = 0.1 M; temperature = $25.0 \pm 0.1^{\circ}C$

b. Refers to total concentration of ligand reactant

For this reaction a wavelength of 254 nm was chosen for study.

In Table 3 are presented the kinetic data which are ordered in terms of increasing hydrogen ion concentration. Within this table are also presented the data for the concentration of the reactive species en, the pseudo-first-order rate constant k^o, and calculated values of $k^o/[en]$. All runs, as previously stated, were conducted at a total en concentration $[en]_T$ in excess over NiEDDA by a factor of at least ten.

Over the pH range studied, ethylenediamine may exist in three distinct forms: en, enH^+, and enH_2^+, with the latter diprotonated species being unreactive. Consequently, for the NiEDDA–en system, there are really two simultaneous reactions leading to the formation of ternary complex:

$$NiEDDA + en \rightleftharpoons NiEDDA(en) \quad , \quad k_{en}^{NiE} \qquad (13)$$

$$NiEDDA + enH^+ \rightleftharpoons NiEDDA(enH)^+ \quad , \quad k_{enH^+}^{NiE} \qquad (14)$$

Furthermore, the kinetic data can be resolved into the rate constants shown in reactions (13) and (14) according to the formula:

$$k^o = k_{en}^{NiE}[en] + k_{enH^+}^{NiE}[enH^+] \qquad (15)$$

For the deprotonation of enH^+,

$$enH^+ \rightleftharpoons en + H^+ \qquad (16)$$

The equilibrium constant[13] is given by:

$$Ka = \frac{[H^+][en]}{[enH^+]} = 1.29 \times 10^{-10} \ M \qquad (17)$$

Solving Eq. (17) for $[enH^+]$ and substituting into Eq. (15) gives:

TABLE 3

Rate Constants for the NiEDDA-en Reaction
($[en]_T$ = 0.025 M)

$[H^+] \times 10^8$ M	$[en] \times 10^3$ M[a]	k^o [b] s^{-1}	$(k^o/[en]) \times 10^{-5}$ $M^{-1}\ s^{-1}$
0.292	1.02	47.3	0.464
0.564	0.525	29.3	0.558
0.611	0.482	32.0	0.664
1.22	0.228	28.2	1.24
3.03	0.0776	23.0	2.97
3.32	0.0675	22.6	3.35
6.50	0.0275	15.0	5.45
7.64	0.0220	14.2	6.45
9.31	0.0162	12.4	7.65
10.2	0.0142	11.6	8.20
10.8	0.0132	11.4	8.77
13.0	0.0975	9.69	9.94
13.5	0.00900	10.0	11.2
15.2	0.00751	9.29	12.4

a. Concentration of free base form of en

b. All runs: I = 0.1 M, T = 25.0 ± 0.1° C

$$k^{o} = k_{en}^{NiE}[en] + k_{enH^+}^{NiE} \frac{[en]}{Ka} [H^+] \qquad (18)$$

Equation (18) is easily rearranged to:

$$\frac{k^{o}}{[en]} = k_{en}^{NiE} + \frac{k_{enH^+}^{NiE}}{Ka} [H^+] \qquad (19)$$

In Figure 2 is shown a plot of the left-hand side of Eq. (19) versus hydrogen ion concentration using the data listed in Table 3. The line represents the least-squares best fit of the data. Thus it appeared possible to find the slope and intercept corresponding to the following terms as given in equation (19):

$$k_{enH^+}^{NiE} / K_a \quad \text{and} \quad k_{en}^{NiE}$$

Rate constants for the reactions of both en and enH^+ can be evaluated from the kinetic data. These values are given in Table 4. Also, in Table 4 are summarized values of the resolved rate constants for other systems involving NiEDDA. For each rate constant listed there is also reported its standard deviation and a correlation coefficient for the appropriate kinetic plot.

NiEDDA-Bipy Reaction

All kinetic runs for the NiEDDA-bipy reaction were performed at a wavelength setting of 305 nm. HEPES buffer (0.01 M) was generally used, except for a few runs in which a H_3BO_3-$Na_2B_4O_7$-mannitol buffer system was employed. The experimental results are provided in Table 5 where the rate constants are arranged according

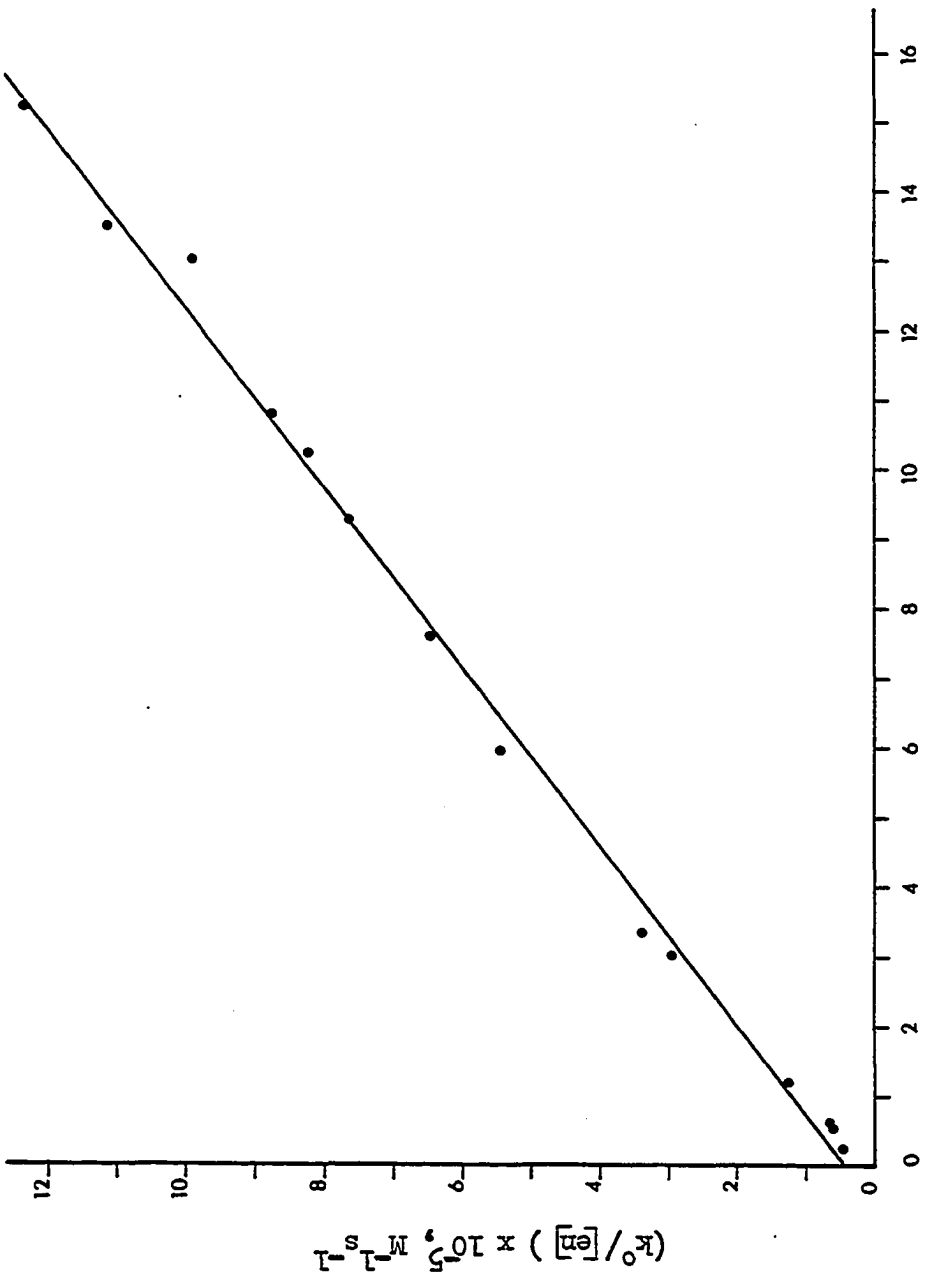

FIGURE 2. Dependence of k^o Upon Hydronium Ion Concentration for the NiEDDA-en Reaction

TABLE 4

Experimental Rate Constants[a] for the Reactions of NiEDDA with EnH^+, Bipy, Phen, Gly, and Sar

Ligand	Rate Constant	Correlation Coefficient
enH^+	$k_f = k^{NiE}_{enH^+} = (1.0 \pm 0.02) \times 10^3\ M^{-1}s^{-1}$	0.998
en	$k_f = k^{NiE}_{en} = (3.4 \pm 1.1) \times 10^4\ M^{-1}s^{-1}$	
bipy	$k_f = k^{bipy}_{NiE} = (5.5 \pm 0.08) \times 10^3\ M^{-1}s^{-1}$	0.999
	$k_b = (8.0 \pm 6.9) \times 10^{-2}\ s^{-1}$	
phen	$k_f = k^{phen}_{NiE} = (4.3 \pm 0.15) \times 10^{+3}\ M^{-1}s^{-1}$	0.994
	$k_b = 3.0 \pm 0.5\ s^{-1}$	
gly	$b = k_2 = 44. \pm 8.0\ s^{-1}$	0.998
	$a = K_1 = 190 \pm 35\ M^{-1}$	
	$k_b = 0.45 \pm 0.06\ s^{-1}$	
sar	$b = k_2 = 44 \pm 11\ M^{-1}s^{-1}$	0.998
	$a = K_1 = 93 \pm 22\ M^{-1}$	
	$k_b = 0.41 \pm 0.06\ s^{-1}$	

a. Uncertainties reported with the rate constants are one standard deviation unit

TABLE 5

Rate Constants k^o for the Reaction of NiEDDA with Bipyridine ($[NiEDDA]_o = 1.51 \times 10^{-4}$ M)

pH	$[bipy]_M \times 10^4$	k^o s^{-1}	Buffer System
8.10	1.50	0.811	Borate
8.01	2.10	1.06	HEPES
8.10	3.00	1.66	Borate
8.01	3.90	2.22	HEPES
8.10	4.50	2.65	Borate
8.01	5.10	2.78	HEPES
7.50	5.10	3.11	Borate
8.01	5.55	3.40	HEPES
8.01	6.00	3.58	HEPES
8.01	6.45	3.79	HEPES
8.01	6.90	3.91	HEPES
7.99	8.40	4.68	HEPES
7.50	10.2	5.63	Borate
7.99	11.4	6.08	HEPES
8.00	12.6	7.04	HEPES
7.98	13.8	7.57	HEPES
7.91	15.0	8.43	HEPES
7.99	17.1	9.64	HEPES

to increasing bipy concentration. In this Table the pH values and the buffer system employed are indicated.

In order to derive a rate constant value for the NiEDDA-bipy reaction, the following procedure was involved. For the purpose of being able to apply the following equations to some of the other kinetic systems studied, let NiC and L represent the nickel(II) complex and ligand respectively. Then the chemical equation for ternary complex formation (written without including charge) is

$$NiC + L \rightleftharpoons NiCL \qquad (20)$$

If the above process is treated as a pseudo-first-order reversible reaction, then the initial rate of decrease of NiC concentration with time is given by:

$$\frac{dx}{dt} = k^{L}_{NiC}([NiC]_o - x)\,[L]_o - k_b x \qquad (21)$$

In this equation, x is the amount of NiC consumed at time t whereas $[NiC]_o$ and $[L]_o$ are the respective initial concentrations of nickel(II) complex and ligand (i.e. NiEDDA and bipy). When the system reaches equilibrium, let x_e represent the amount of nickel complex that has been lost, so that Eq. (21) is readily simplified and solved for k_b:

$$k_b = \frac{k^{L}_{NiC}[L]_o([NiC]_o - x_e)}{x_e} \qquad (22)$$

Substituting this latter equation into Eq. (21) gives

$$\frac{dx}{dt} = k^{L}_{NiC}[L]_o([NiC]_o - x) - \frac{k^{L}_{NiC}[L]_o}{x_e}(NiC_o - x_e)\frac{x}{x_e} \qquad (23)$$

Eq. (23) is easily rearranged to integral form:

$$\int_{o}^{x} \frac{x_e\,dx}{NiC\,(x_e-x)} = \int_{o}^{t} k\,dt \qquad (24)$$

Integration of the latter equation with respect to x and t, followed by simplification yields:

$$k^{L}_{NiC}\,L_o + k_b = \frac{-1}{t} \ln \frac{[NiCL]_e - [NiCL]}{[NiC]_e - [NiC]_o} \qquad (25)$$

From the above equation, a new rate coefficient k^o representing the left-hand side can be defined:

$$k^o = k^{L}_{NiC}[L]_o + k_b \qquad (26)$$

This rate constant k^o is the measured value, obtained under pseudo-first-order conditions, and is the one presented in Table 5. A plot of k^o versus ligand concentration is shown in Figure 3. Thus it appears that Eq. (26) satisfactorily represents the data. The slope and intercept of this plot correspond to k^{bipy}_{NiE} and k_b respectively. These latter resolved rate constants are listed in Table 4.

NiEDDA-Phen Reaction

The rate measurements for this system were obtained at 343 nm, except for the runs in the 5.0×10^{-4} to 9.9×10^{-4} M concentration range, for which a wavelength of 327 nm was used. This latter wavelength provided better data in the lower concentration range. The kinetic data are summarized in Table 6 in which the buffer system used is indicated.

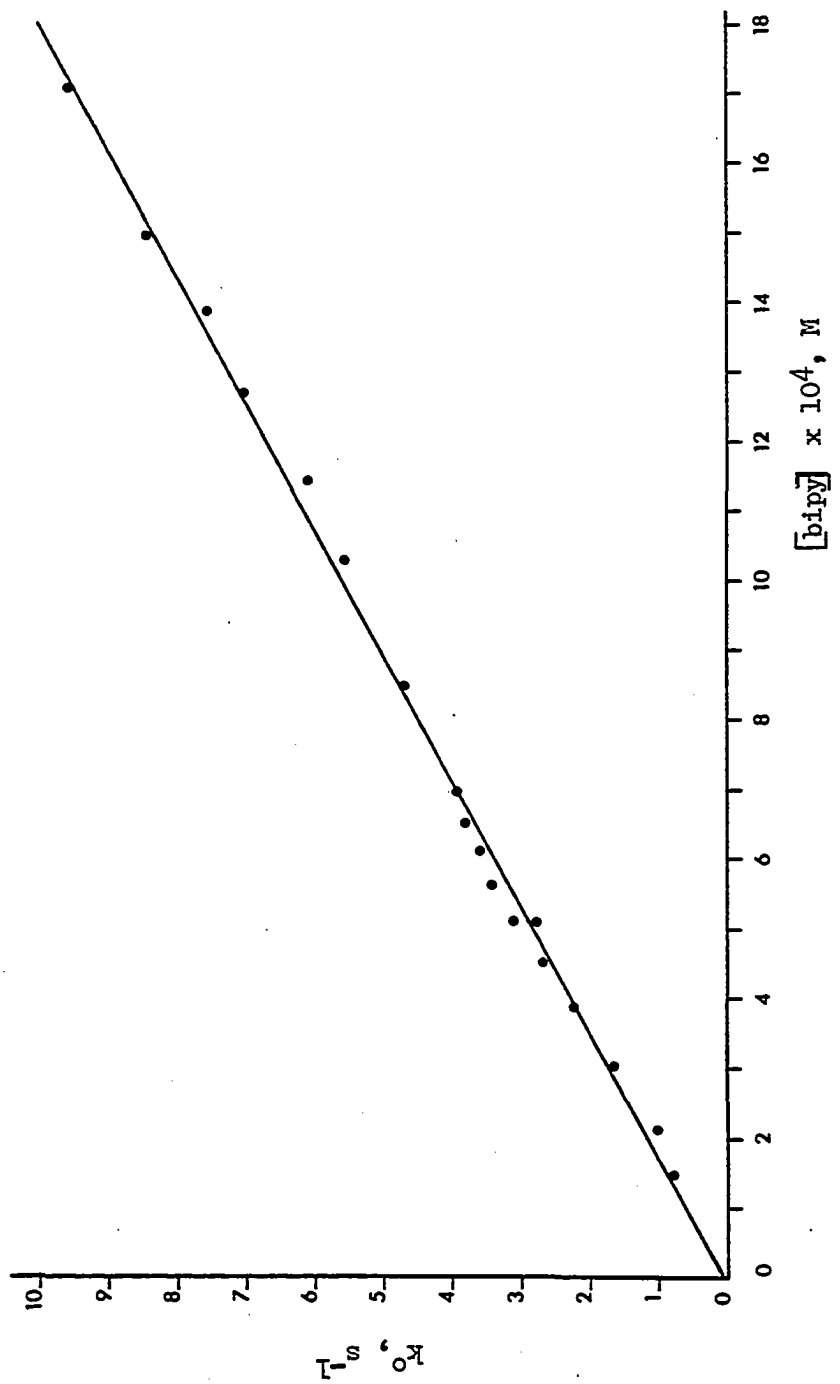

FIGURE 3. Dependence of k^o Upon Bipy Concentration for the NiEDDA-bipy Reaction

TABLE 6

Experimental Values of the Rate Constants for the NiEDDA-Phen Reaction[a]

pH	$[Phen]_M \times 10^3$	$k^o_{s^{-1}}$[b]	Buffer System
7.99	0.51	3.68	HEPES
8.00	0.75	5.63	HEPES
8.01	0.99	7.25	HEPES
8.49	1.51	9.51	Borate
8.01	1.76	11.6	HEPES
8.01	2.51	14.5	HEPES
8.00	3.00	16.4	Borate
7.50	3.00	16.8	Borate
8.00	3.60	18.8	HEPES
8.00	4.50	23.4	HEPES
8.00	5.25	24.9	HEPES
8.00	6.00	27.6	HEPES

a. HEPES buffer at 0.01 M

$[NiEDDA]_o = 1.51 \times 10^{-4}$ M

b. All runs: T = 25.0° C, I = 0.1 M

The kinetics of the NiEDDA-phen reaction appeared to follow the expressions (21) and (26), as presented in the previous section for the NiEDDA-bipy system. A plot of the measured rate constant versus phen concentration is shown in Figure 4. The plot is linear over the entire concentration range of phen which was varied by a factor of 12. Moreover, the value of the rate constant k^{o} was independent of either pH or the buffer system employed. The values of the rate constants k_{NiE}^{bipy} and k_{b} are listed in Table 4.

NiEDDA-Glycine Reaction

The wavelength chosen for study of the reaction between NiEDDA and glycine was 240 nm. The reaction was examined over the pH range 6.8 to 9.1 using both HEPES and TAPS buffers at a concentration of 0.1 M. In all cases, the total glycine concentration was in at least a 10-fold excess over the NiEDDA concentration. Several preliminary experiments were performed in order to test whether the buffers used affected the measured values of the rate constants under pseudo-first-order conditions. These experiments were performed over a range of buffer concentrations from 0.01 to 0.125 M, at an ionic strength of 1.2 M for TAPS buffer and 0.1 M for HEPES buffer. The results of the preliminary runs are given in Table 7. Figure 5 is a plot of k^{o} against buffer concentration, for both HEPES and TAPS buffers. Within experimental error, the rate constant does not appear to be a function of buffer concentration.

All of the data for the NiEDDA-glycine system are collected in Table 8, where the data are first ordered in terms of increasing

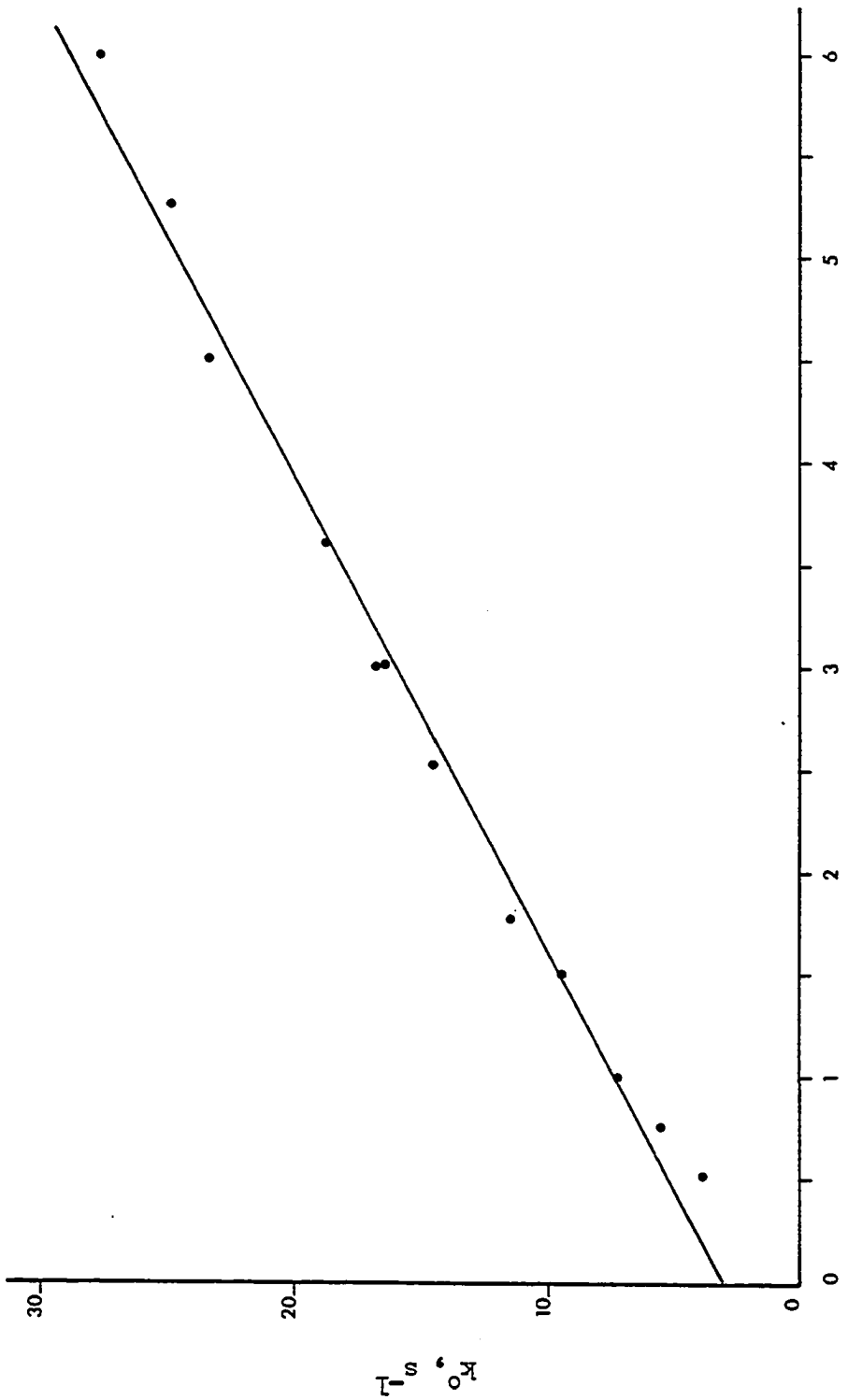

FIGURE 4. Plot of k^o Versus Phen Concentration for the NiEDDA-phen System

TABLE 7

Experimental Conditions and Rate Constants for the Reactions of NiEDDA and Glycine ($[gly]_o$ = 0.01 M)

pH	Buffer Concentration, M	I M	k^o s^{-1}
8.03	0.025[a]	0.1	1.91
8.02	0.050[a]	0.1	2.00
8.03	0.075[a]	0.1	1.93
8.01	0.10[a]	0.1	1.98[c]
7.98	0.01[b]	1.2	4.66
7.97	0.025[b]	1.2	4.68
8.02	0.060[b]	1.2	4.35
8.01	0.090[b]	1.2	4.75
8.01	0.125[b]	1.2	4.82[d]

a. HEPES buffer, $[NiEDDA]_o = 7.56 \times 10^{-4}$ M

b. TAPS buffer, $[NiEDDA]_o = 8.02 \times 10^{-4}$ M

c. Average k for I = 0.1 M Runs, $k^o = 1.96 \pm 0.042$ s^{-1}

d. Average k for I = 1.2 M Runs, $k^o = 4.65 \pm 0.18$ s^{-1}

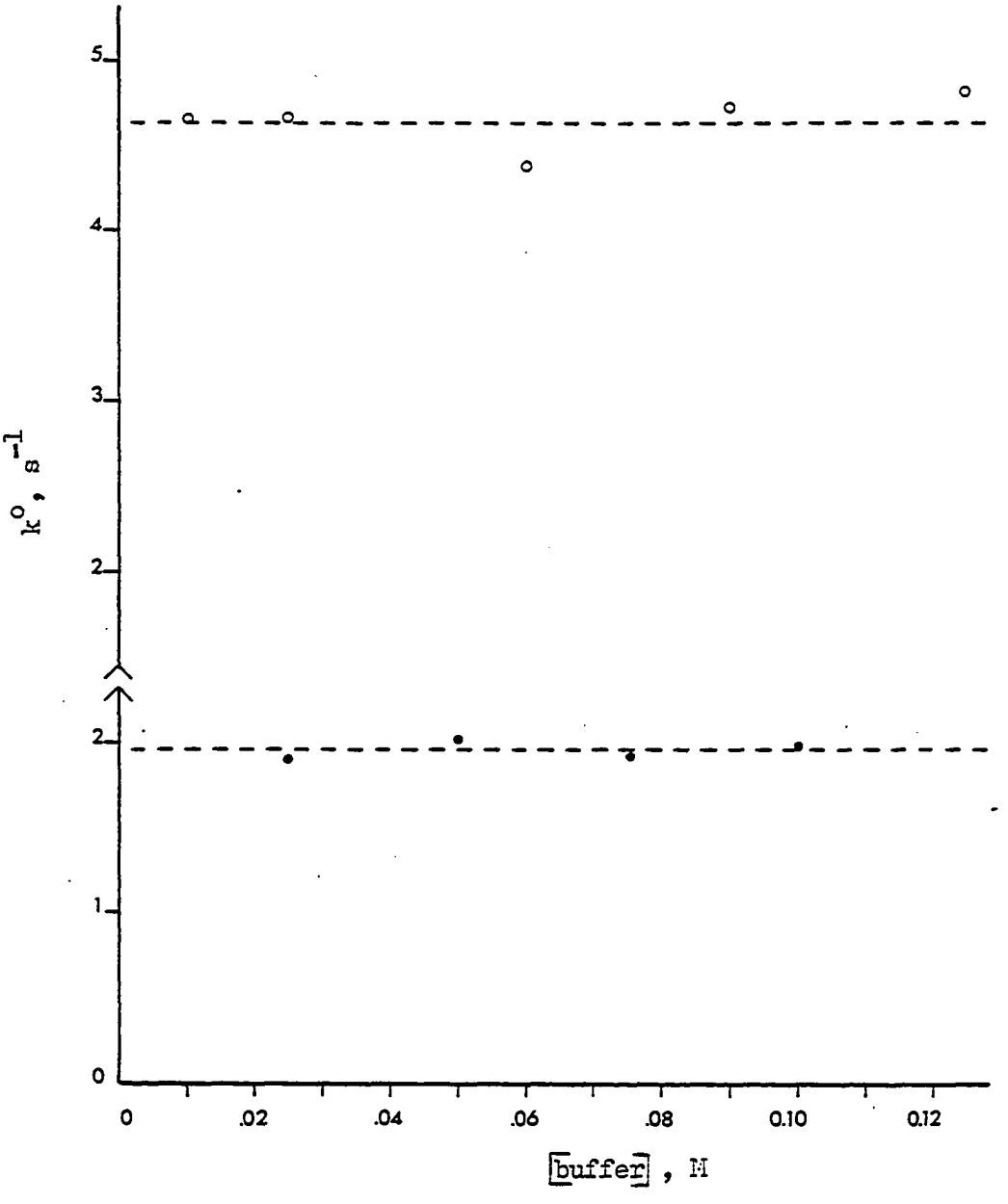

FIGURE 5. Plot of k^o vs. Buffer Concentration for the NiEDDA-Gly Reaction; Upper Line is for TAPS Buffer, Lower Line is for HEPES Buffer

TABLE 8

Experimental Values of Rate Constants for the Reaction Between NiEDDA and Glycine ($[NiEDDA]_o = 1.12 \times 10^{-3}$ M Except Run Marked * for Which $[NiEDDA]_o = 1.25 \times 10^{-3}$ M)

pH	$[gly] \times 10^2$ M	$[gly^-] \times 10^4$ M	k^o s^{-1}
6.83	1.30	0.235	0.646
6.85	1.60	0.305	0.610
6.83	3.20	0.578	0.862
6.83	5.00	0.916	1.10
6.83	7.50	1.37	1.40
6.83	10.0	1.81	1.77
7.02*	2.00	0.557	0.850
7.02	5.00	1.39	1.66
7.02	7.00	1.96	2.14
7.01	10.0	2.74	2.82
7.19	1.30	0.544	0.894
7.22	1.60	0.711	0.903
7.23	3.20	1.46	1.84
7.22	5.00	2.21	2.31
7.23	7.50	3.41	3.14
7.23	10.0	4.53	3.94
7.50	1.30	1.04	1.29
7.51	3.20	2.74	2.57

TABLE 8 (continued)

7.51	5.00	4.28	3.63
7.52	7.50	6.59	4.83
7.50	10.0	8.47	6.16
7.64	1.60	1.85	1.94
7.77	1.30	2.04	2.11
7.78	3.20	5.08	4.66
7.78	5.00	7.90	6.39
7.78	7.50	12.0	8.76
7.78	10.0	16.1	9.94
7.81	1.60	2.76	2.75
7.83	1.60	2.84	2.57
8.01	1.60	4.30	3.92
8.23	1.60	7.02	5.93
8.39	4.80	29.5	16.5
8.39	6.20	38.2	20.6
8.40	7.70	48.7	21.5
8.41	1.60	10.3	8.94
8.45	1.60	11.3	8.86
8.56	1.60	14.2	10.8
8.59	4.30	40.7	18.4
8.59	4.60	43.8	21.5
8.60	3.50	34.1	16.1
8.67	1.60	17.8	12.1

TABLE 8 (continued)

8.77	1.60	21.8	14.7
8.83	1.60	24.5	16.2
8.91	1.60	28.7	17.8
9.03	1.60	35.6	18.7
9.08	1.60	39.0	16.2

a. Calculated from pK_a of glycine[13]

pH, and secondly according to increasing [gly] at constant pH. An analysis of the kinetic data proceeded as follows. First of all, it was assumed that glycinate ion was the only reactive species, as was found for the reaction of $Ni(trien)^{2+}$ and glycine. In order to generalize the following discussion, let L^- represent the concentration of gly^-. Then the equation for ternary complex formation can be written:

$$NiEDDA + L^- \rightleftharpoons NiEDDA(L^-) \qquad (27)$$

Letting NiC represent the concentration of nickel chelate (in this case NiEDDA), the equilibrium constant for Eq. (27) is written as

$$K_a = \frac{[NiCL]}{[NiC][L^-]} \qquad (28)$$

The rate law that described the decrease in NiEDDA concentration with time appeared to be:

$$\frac{-d[NiC]}{dt} = k^L_{NiC}[NiC][L] - k_b[NiCL] \qquad (29)$$

The above expression represents a pseudo-first-order reversible reaction whose forward and reverse rate constants are given by k^{L}_{NiC} and k_b. The integrated form of Eq. (29) is of the same form as equation (25) of the NiEDDA-bipy section. According to this latter equation, the experimentally determined pseudo-first-order rate constant k^{o} can be defined as

$$k^{o} = k^{L}_{NiC}[L] + k_b \qquad (30)$$

In Figure 6 are shown plots of k^{o} versus total glycine concentration at constant pH. From these plots it is apparent that k^{o} shows a good first-order dependence on glycine concentration up to a pH value of 7.2. However above this latter pH value, the plots became nonlinear with respect to total glycine concentration, indicating that equation (30) was no longer valid. The foregoing dependence of k^{o} on total glycine concentration corresponds to a shift in reaction order (with respect to gly) from one to zero, if as it appears in Figure 6, that the curves at high pH will level off.

Another feature of the family of curves illustrated in Figure 6 is that each one appears to have the same intercept. When a least squares procedure was applied to the lines (below pH 7.5), an average value for k_b of Eq. (30) was obtained as 0.45 s^{-1}. When k_b is subtracted from k^{o}, a value for the forward rate constant, k^{o}; is obtained. Figure 7 shows a plot of k^{o}; versus $[gly^{-}]$ which was varied by a factor of about 250. From the data plotted in Figure 7, it appears that all points covering all pH values and gly^{-} concentrations, can be represented by the same curve. This

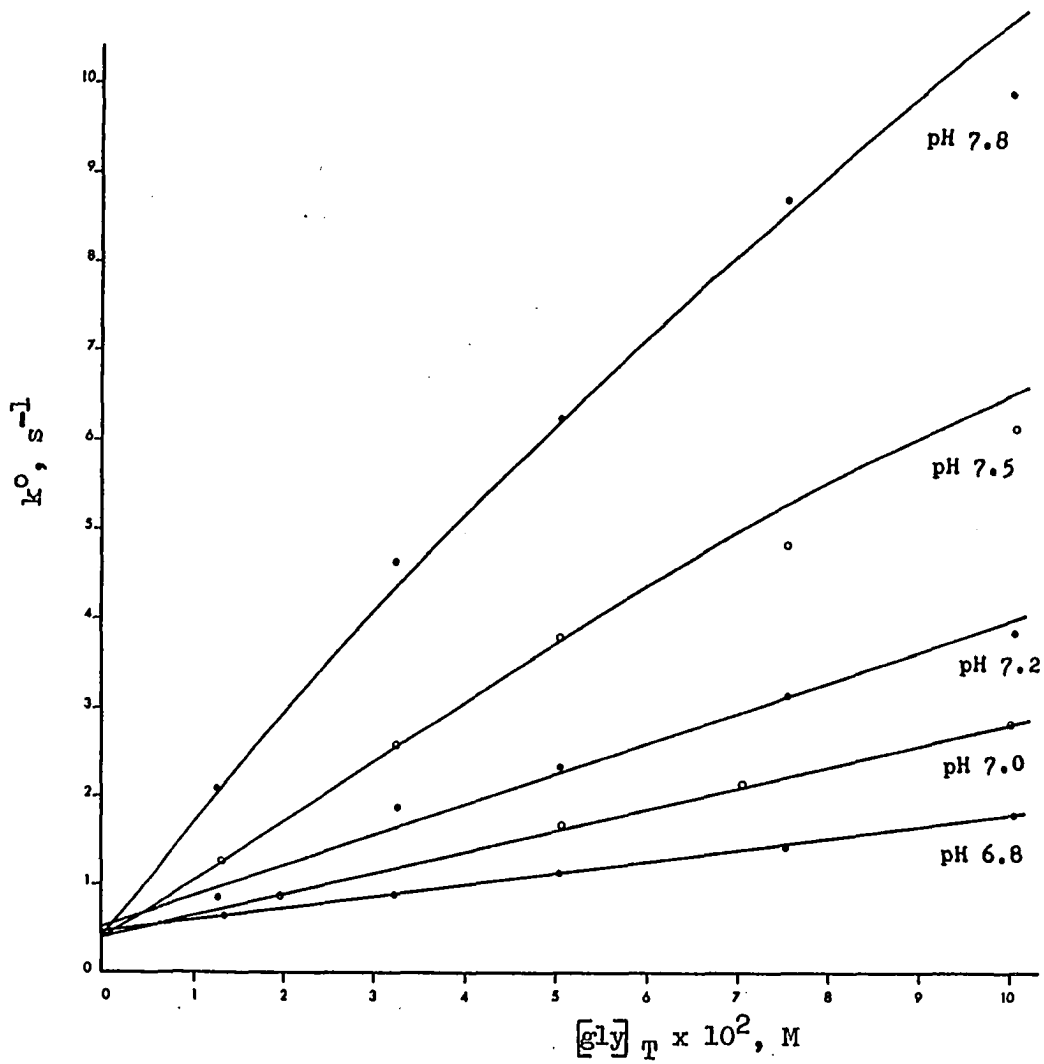

FIGURE 6. Dependence of k^o Upon Total Glycine Concentration; Lines Below pH 7.5 are Least-Squares Best Fits

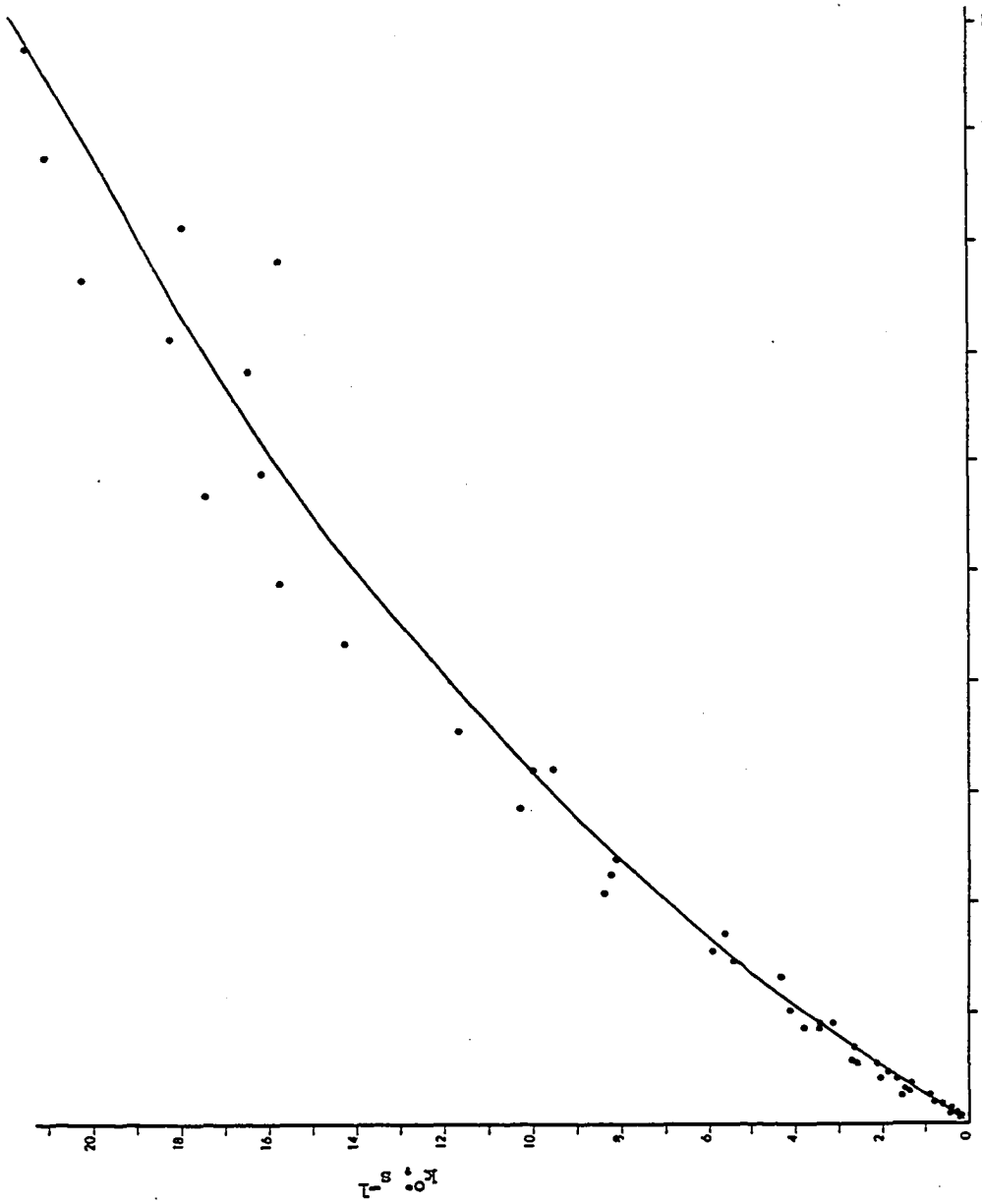

FIGURE 7. Variation of $k^{o'}$ With Gly^- Concentration Over the pH Range 6.8 to 9.0. Curve is Calculated From Equation (31)

curve appears to be linear at low gly^- concentrations, but gradually curves and finally appears to level off at high gly^- concentrations. The behavior displayed in Figure 7 provides further evidence that the reaction order with respect to gly^- changes from first to zero as the glycinate ion concentration increases. An empirical equation that describes the variation of $k^{o\bullet}$ with $[gly^-]$, illustrated in Figure 7, is

$$k^{o\bullet} = \frac{ab[L^-]}{1 + a[L^-]} \qquad (31)$$

In this latter equation, as stated before, $[L^-]$ represents gly^- concentration. In addition, this equation is easily rearranged to linear form:

$$1/k^{o\bullet} = \frac{1}{ab[L^-]} + \frac{1}{b} \qquad (32)$$

Figure 8 illustrates a plot of equation (32) over the gly^- concentration range 1.85×10^{-4} to 4.87×10^{-3} M. From this plot the values of a and b were found from the slope and intercept of Eq. (32). These values are given in Table 4 along with the value of k_b.

NiEDDA-Sarcosine Reaction

The reaction of NiEDDA and sarcosine was studied at wavelength 242 nm. Both HEPES and TAPS buffers were employed over the pH range 6.8 to 9.1 at 0.1 M concentration. Table 9 summarizes the experimental data whose treatment is similar to that employed for the NiEDDA-glycine reaction. Figure 9 shows plots of the measured rate

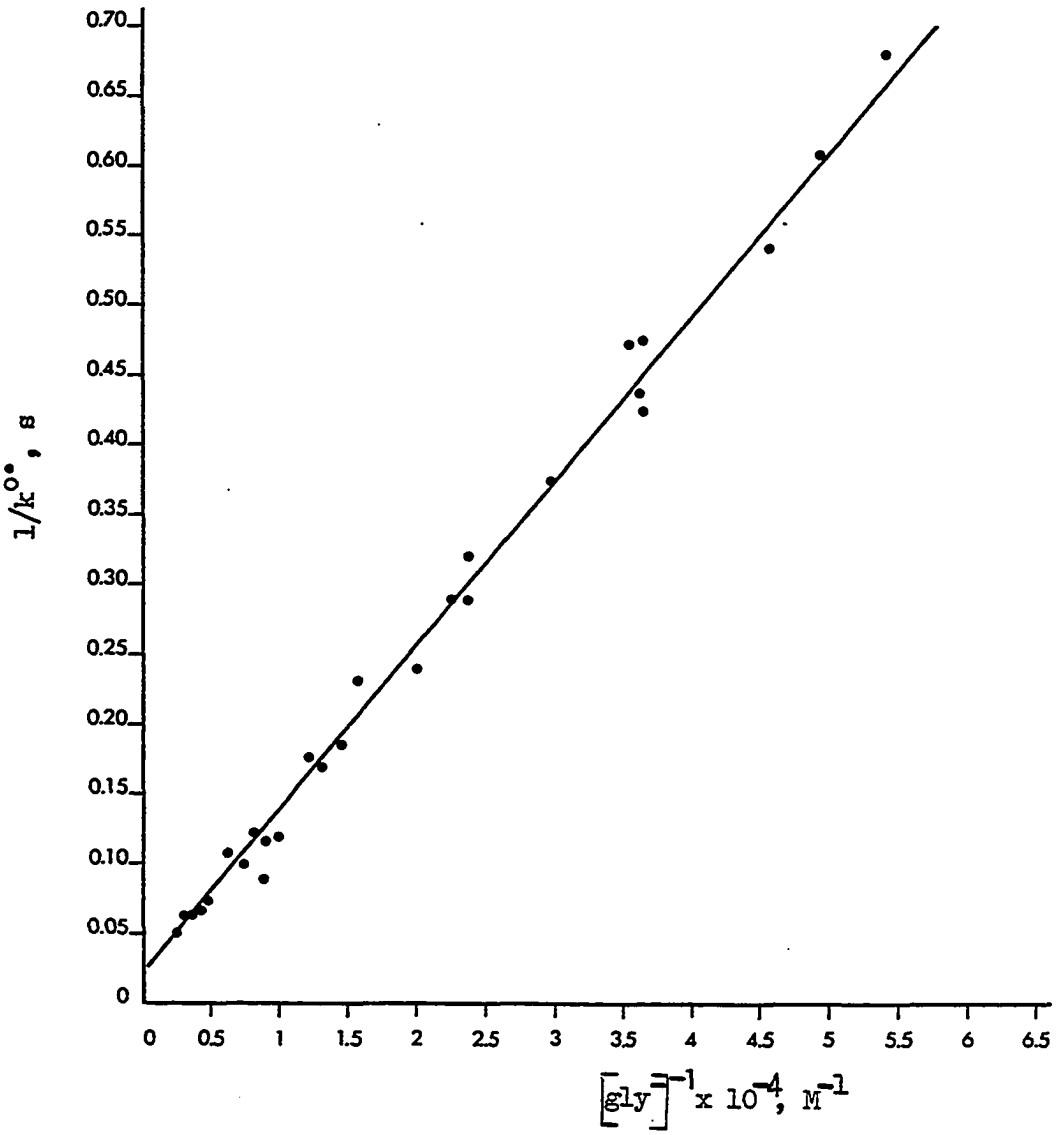

FIGURE 8. Resolution of $k^{o\bullet}$ for the NiEDDA-Gly Reaction. Plot Covers Gly^- Concentration Range of 1.8×10^{-4} to 4.9×10^{-3} M

TABLE 9

Experimental Conditions and Rate Constants for the Reaction Between NiEDDA (NiE) and Sarcosine

pH	$[NiE] \times 10^3$ M	$[sar] \times 10^2$ M	$[sar^-] \times 10^4$ M	k^o s^{-1}
6.86	1.28	2.00	0.148	0.470
6.85	1.28	3.50	0.252	0.470
6.86	1.28	7.00	0.512	0.540
6.85	1.28	9.00	0.658	0.580
7.22	1.12	1.60	0.273	0.413
7.21	1.28	1.80	0.298	0.532
7.21	1.28	3.00	0.495	0.534
7.21	1.28	4.50	0.742	0.705
7.21	1.28	7.00	1.15	0.773
7.21	1.28	8.00	1.33	0.883
7.20	1.28	10.6	1.71	1.01
7.42	1.12	1.60	0.428	0.443
7.62	1.12	1.60	0.681	0.531
7.76	1.28	1.30	0.754	0.587
7.81	1.12	1.60	1.04	0.740
7.81	1.16	1.70	1.12	0.770
7.75	1.28	1.80	1.03	0.826
7.74	1.28	3.60	2.03	1.25

TABLE 9 (continued)

7.74	1.28	6.00	3.39	1.79
7.74	1.28	9.00	5.06	2.55
7.74	1.28	1.09	6.14	2.68
7.99	1.28	1.80	1.79	1.07
7.99	1.28	5.00	4.98	2.28
7.97	1.28	7.50	7.13	3.00
7.97	1.28	10.0	9.50	4.32
7.98	1.28	11.0	10.6	4.75
8.01	1.12	1.60	1.65	0.917
8.16	1.12	1.60	2.33	1.23
8.21	1.12	1.60	2.61	1.44
8.39	1.12	3.40	8.26	3.53
8.42	1.12	1.60	4.19	2.07
8.61	1.12	1.60	6.44	2.67
8.59	1.12	5.00	19.1	7.00
8.60	1.12	5.60	21.8	7.84
8.59	1.12	7.50	28.6	9.72
8.58	1.12	10.0	37.4	12.3
8.81	1.12	1.60	9.89	4.16
8.81	1.12	4.00	24.7	9.09
8.79	1.35	6.00	35.9	11.3
8.79	1.35	7.00	41.6	13.6
8.79	1.35	8.00	47.2	14.8
8.81	1.35	9.00	55.4	16.4

TABLE 9 (continued)

8.89	1.12	1.60	11.9	5.21
9.03	1.12	1.60	16.9	6.32
9.07	1.12	1.70	17.1	6.48

constant vs. total sarcosine concentration at constant pH. The rate constant k^{o} is a linear function of $[sar]_T$ for pH values below 8 whereas above this value, the dependence of k^{o} on $[sar]_T$ was non-linear. These changes appear to indicate a change in reaction order with respect to $[sar]_T$, as the total sar concentration is increased. From Figure 9, the average intercept k_b was obtained as 0.410 s^{-1}. A value for the forward rate constant k^{o*}, was obtained by subtracting k_b from k^{o}. Figure 10 illustrates a plot of k^{o*} versus $[sar^{-}]$ over the concentration range 1.15×10^{-3} to 5.54×10^{-1} M. All points throughout this latter concentration range appeared to be represented by the same curve. When the intercept k_b was subtracted from k^{o*}, and the data plotted according to equation (32), the constants a and b could be directly obtained from the values of the slope and intercept. The corresponding plot is shown in Figure 11; the derived rate constants are given in Table 4.

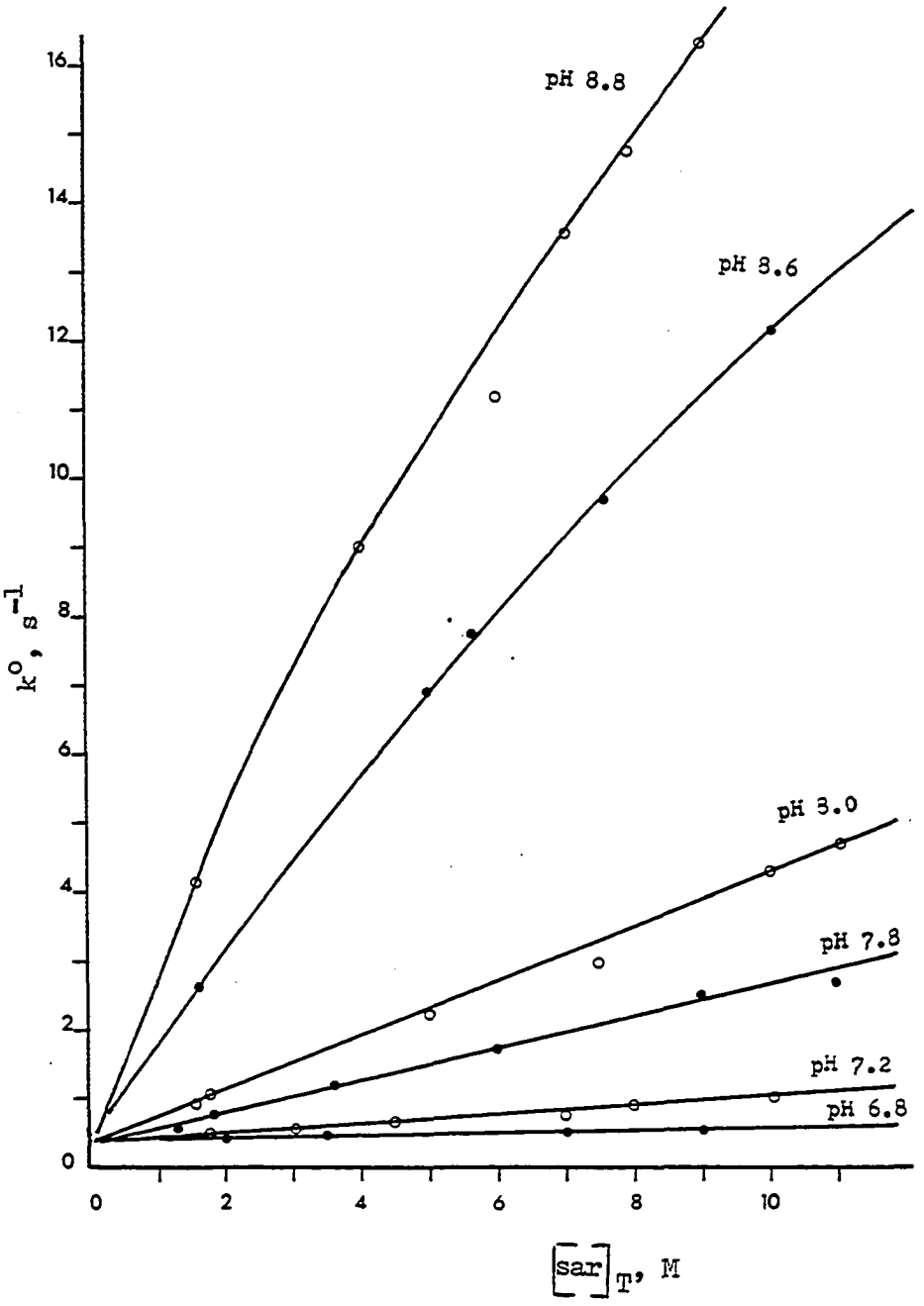

FIGURE 9. Effect of Sar Concentration on k^o for the NiEDDA-sar Reaction; Lines below pH 8.6 are Least-Squares - Best Fits

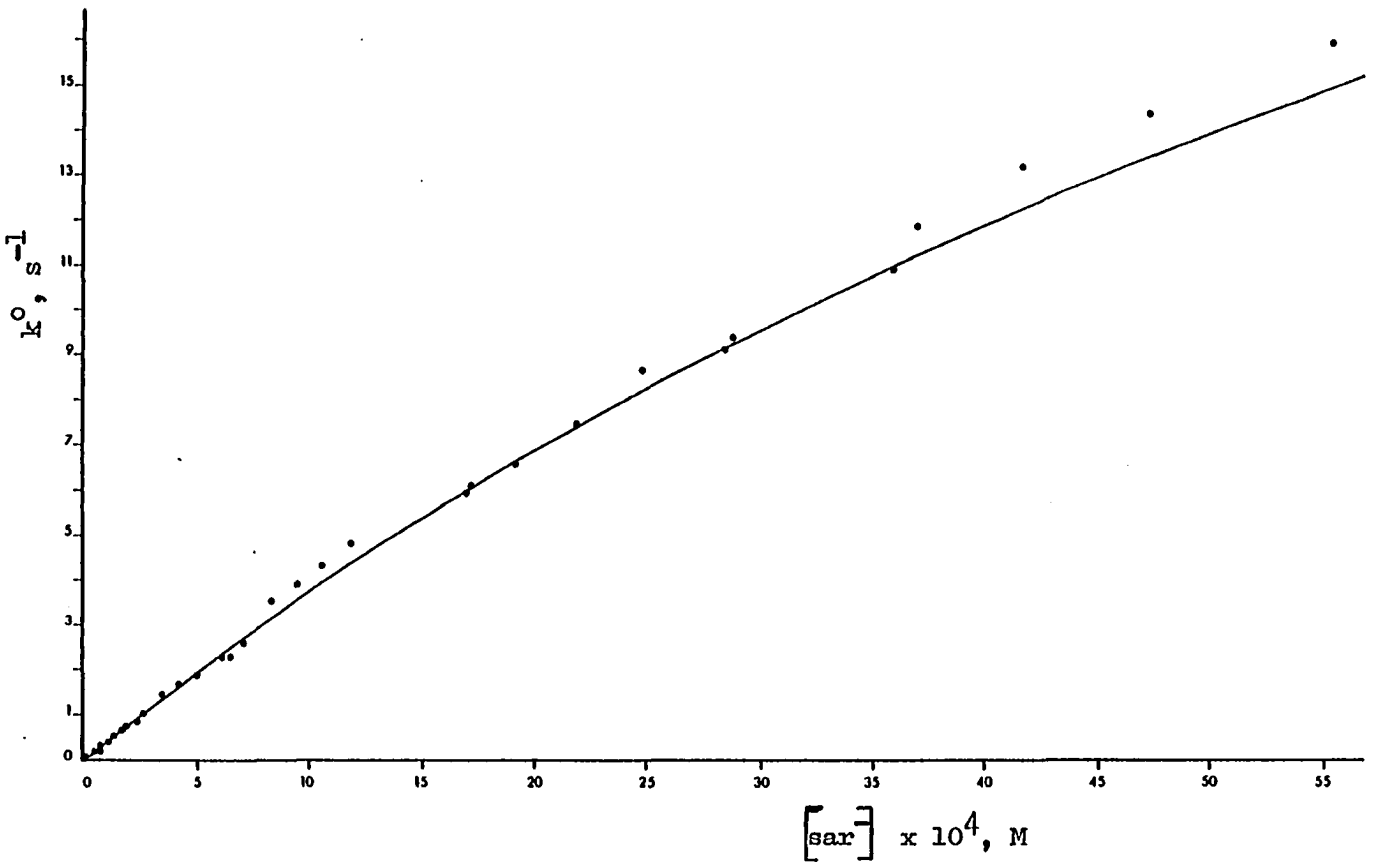

FIGURE 10. Variation of $k^{o'}$ With Sar^- Concentration for the NiEDDA-sar^- Reaction; Curve is Calculated from Equation (31)

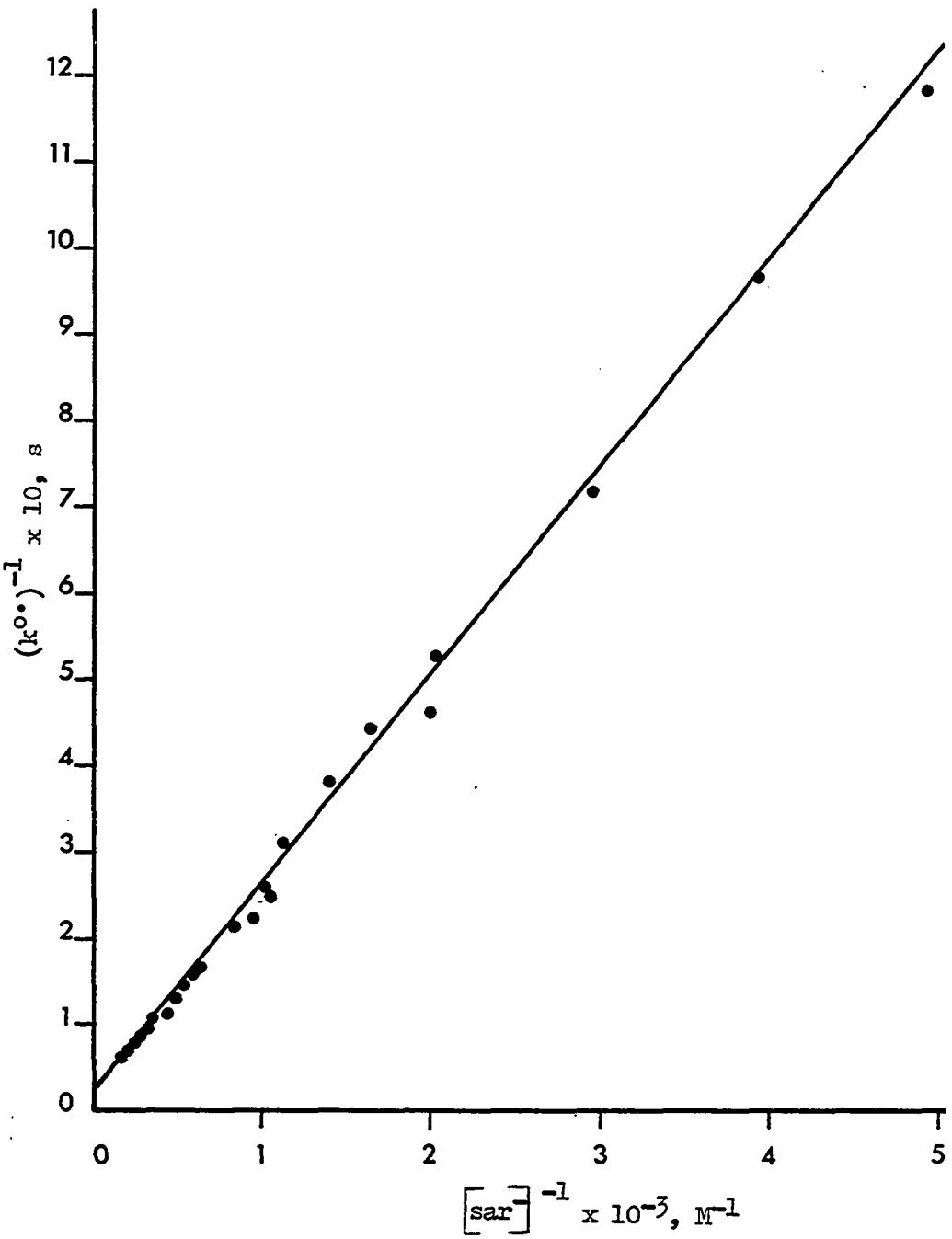

FIGURE 11. Resolution of $k^{o\bullet}$ into a and b for the NiEDDA-sar Reaction; Plot Covers Sar^{-} Concentration Range of 2.03×10^{-4} to 5.54×10^{-3} M

Kinetic Systems Involving $Ni(trien)^{2+}$

$Ni(trien)^{2+}$-En Reaction

The reaction between $Ni(trien)^{2+}$ and en was monitored at a wavelength of 252 nm, over the pH range 6.9 to 8.9. Both HEPES and TAPS buffers were employed at a concentration of 0.1 M. Table 10 lists the kinetic data, ordered in terms of increasing hydrogen ion concentration $[H^+]$.

The essentials of the ternary complex formation for this system are analogous to those of the NiEDDA-en system, except for the +2 charge of the complex. Furthermore, a rate expression analogous to Eq. (19) can be written for the $Ni(trien)^{2+}$-en system:

$$\frac{k^{o}_{NiT}}{[en]} = k^{NiT}_{en} + \frac{k^{NiT}_{enH^+}}{Ka}[H^+] \qquad (33)$$

According to the above equation, a plot of the left-hand side versus $[H^+]$ should give a straight line whose slope and intercept are identified by the terms

$$\frac{k^{NiT}_{enH^+}}{Ka} \quad \text{and} \quad k^{NiT}_{en}$$

A plot of the data given in Table 10 is shown in Figure 12. The data appears to follow equation (33). The least-squares method was employed to obtain values of the slope and intercept. However, the uncertainty in the intercept is so large that it can not be distinguished from zero. The value of the $k^{NiT}_{enH^+}$ and its uncertainty is given in Table 11. In addition, this Table lists resolved rate constants

TABLE 10

Experimental Rate Constants For the $Ni(trien)^{2+}$-Ethylenediamine Reaction ($[en]_T$ = 0.0589 M)

$[H^+] \times 10^8$ M	$[en] \times 10^5$ M[a]	k^o [b,c] s^{-1}	$(k^o/[en]) \times 10^{-5}$ $M^{-1} s^{-1}$
0.130	523.	69.5	0.133
0.470	149.	70.5	0.473
1.04	64.2	64.3	1.00
2.00	30.5	58.9	1.93
3.07	18.0	50.5	2.91
4.85	9.84	42.7	4.34
6.92	6.01	40.2	6.78
8.63	4.30	37.5	8.97
11.4	2.83	31.0	11.0
12.5	2.42	29.8	12.2

a. Concentration of free base form of en

b. All runs: I = 0.1 M, T = 25.0 ± 0.1° C

c. $Ni(trien)^{2+}$ concentration at 1.51×10^{-3} M

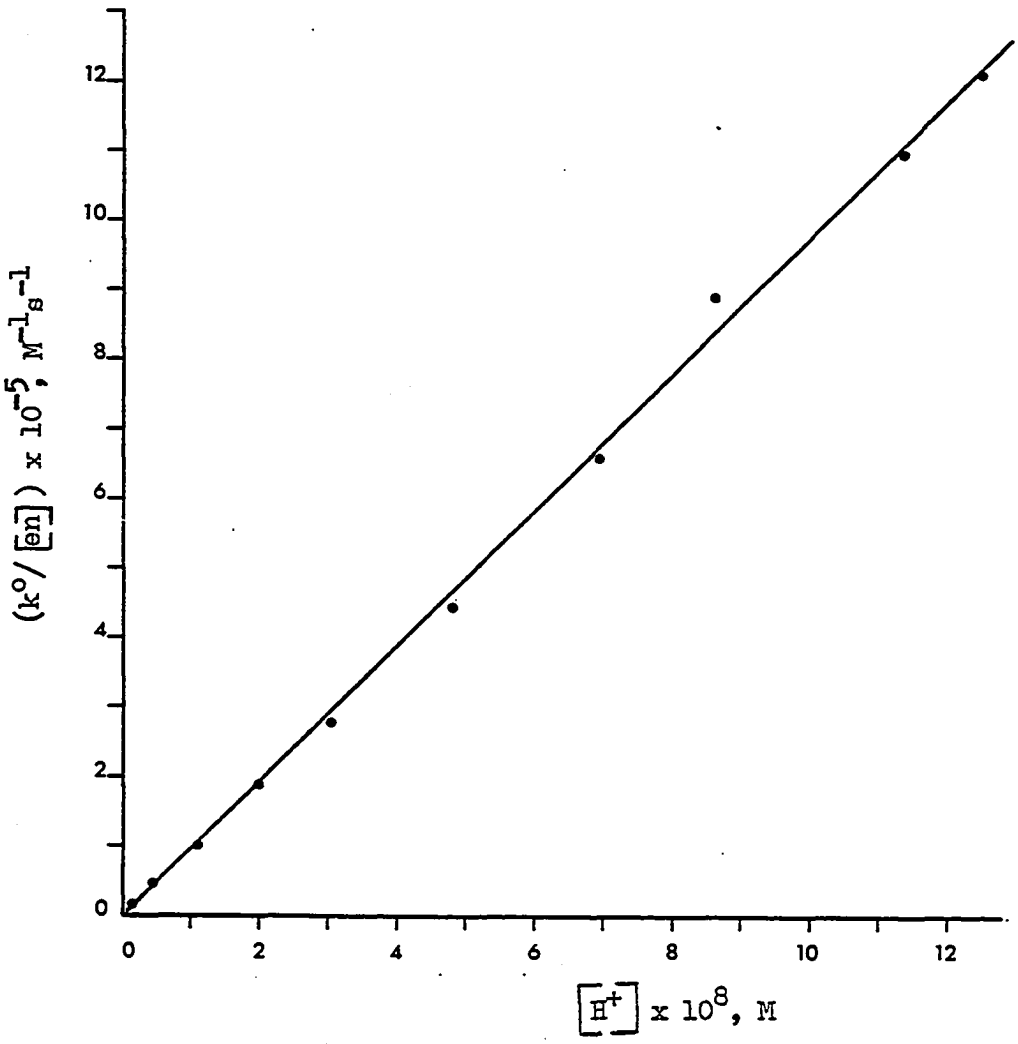

FIGURE 12. Plot of $k^o_{NiT}/[en]$ vs. $[H^+]$ for the $Ni(trien)^{2+}$-en Reaction

TABLE 11

Experimental Rate Constants for the Reactions of $Ni(trien)^{2+}$ with EnH^+, Bipy, Phen, and Sar

Ligand	Rate Constant [a]	Correlation Coefficient
enH^+	$k_f = k_{enH^+}^{NiT} = (1.3 \pm .023) \times 10^{+3}\ M^{-1}s^{-1}$	0.999
bipy	$k_f = k_{NiT}^{bipy} = (7.6 \pm 0.15) \times 10^{+3}\ M^{-1}s^{-1}$	0.998
	$k_b = 0.18 \pm 0.06\ s^{-1}$	
phen	$k_f = k_{NiT}^{phen} = (8.2 \pm 0.16) \times 10^{3}\ M^{-1}s^{-1}$	0.997
	$k_b = 5.3 \pm 0.51\ s^{-1}$	
sar	$b = k_2 = 68 \pm 66\ s^{-1}$	0.940
	$a = K_1 = 430 \pm 415\ M^{-1}$	
	$k_b = 17.7 \pm 0.28\ s^{-1}$	

a. Uncertainties reported with the rate constants are one standard deviation unit

for the reactions of $Ni(trien)^{2+}$ with other bidentate ligands, as described in the following sections.

$Ni(trien)^{2+}$-Bipy Reaction

The kinetic system involving $Ni(trien)^{2+}$ and bipy was monitored at a wavelength of 305 nm. All solutions were buffered using HEPES, at pH values of 7.4 and 8.0. The measured values of the pseudo-first-order rate constants, k^o, are listed in Table 12, in terms of increasing bipy concentration. Analysis of the rate behavior of the above system was analogous to that previously described for the NiEDDA-bipy system. Thus equations (21) and (26) were employed to resolve the rate constants for this system. A plot of k^o vs. [bipy] according to equation (26) is shown in Figure 13. The linear-least-squares method was used to deduce values of the slope k_{NiT}^{bipy} and intercept k_b. These latter values are listed in Table 11.

$Ni(trien)^{2+}$-phen reaction

Several rate measurements were performed on the $Ni(trien)^{2+}$-phen system, and the results were combined with those previously reported by Steinhaus and Lee[12]. These latter data were obtained at pH values of 7.1 and 7.5, with and without the use of buffer. The present series of kinetic runs were performed at pH 8.0, using HEPES buffer at 0.01 M. The wavelength used for this study was 327 nm.

All of the kinetic data are collected in Table 13. The data were treated according to equations (21) and (26). Figure 14 shows a plot of k^o versus [phen], according to Eq. (26). The plot appears

TABLE 12

Rate Constants for the Reaction of $Ni(trien)^{2+}$ With Bipyridine Using HEPES Buffer at 0.01 M ($[Nitrien]_o = 1.67 \times 10^{-5}$ M)

pH	$[bipy]_M \times 10^4$ [b]	k^o [a] s^{-1}
7.41	1.80	1.50
7.98	3.00	2.20
7.40	3.00	2.36
7.39	4.44	3.45
7.40	6.15	4.72
7.98	7.50	5.81
7.41	9.00	7.35
8.00	11.1	9.00
8.00	14.1	11.2
7.99	17.1	13.3
8.01	20.1	15.0

a. All runs: I = 0.1 M, T = 25.0 ± 0.1° C

b. pK_a value of bipy given in reference 13

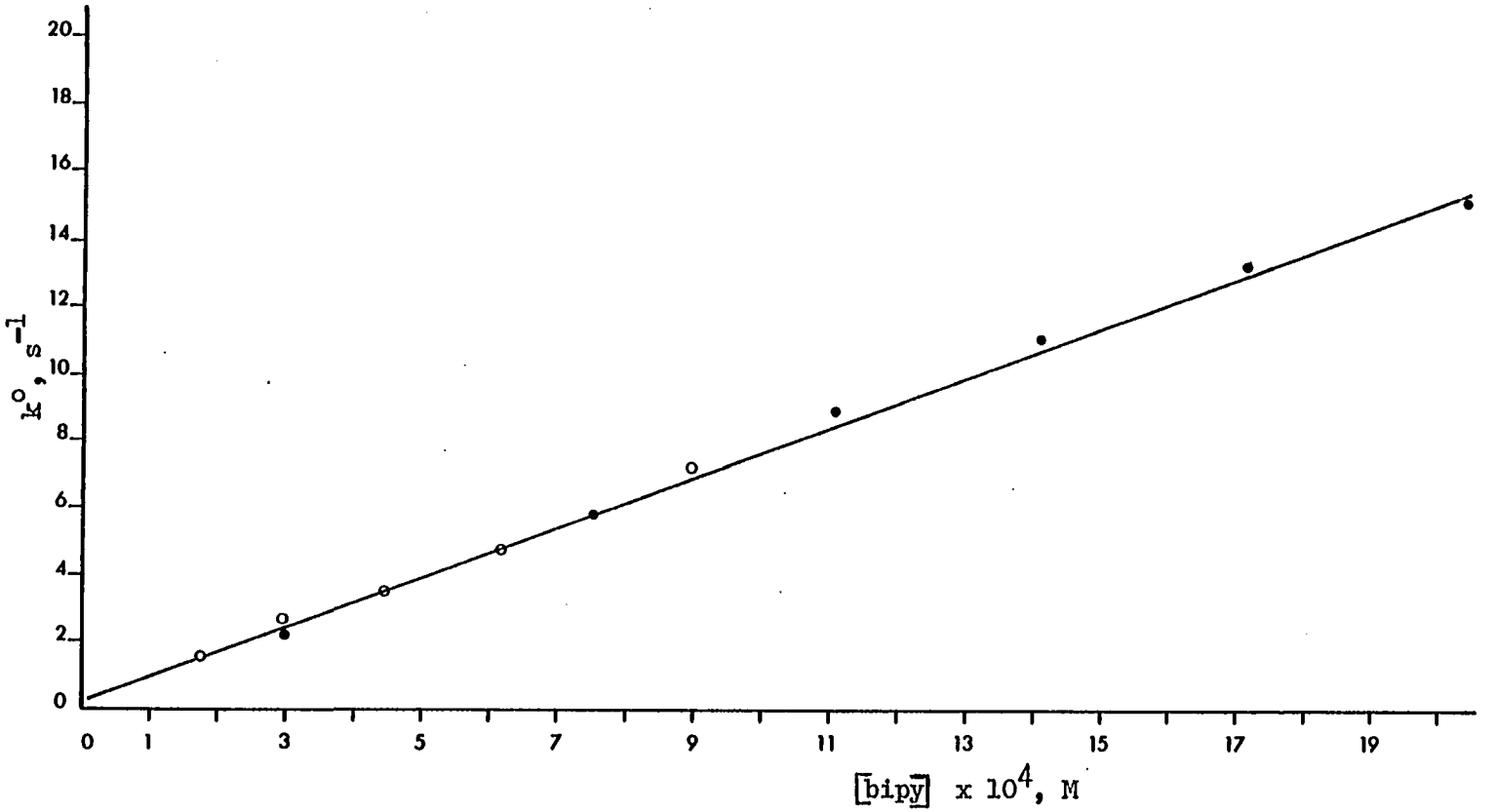

FIGURE 13. Dependence of k^o on Bipy Concentration for the $Ni(trien)^{2+}$ - bipy Reaction. Points Marked o are at pH 7.4, • for pH 8.0

TABLE 13

Rate Constants for the Reaction Between $Ni(trien)^{2+}$ and 1,10-Phenanthroline (HEPES Buffer at 0.01 M)

pH	$[Ni(trien)^{2+}]_M \times 10^4$	$[phen]_M \times 10^3$	k^o_{-1} s^{-1}
7.99[a]	0.204	0.210	6.15
7.99[a]	0.464	0.540	10.6
8.00[a]	0.464	0.720	12.7
8.00[a]	0.464	0.900	13.3
7.12[b]	1.44	1.49	16.0
7.49[b]	1.44	1.50	17.2
7.11[b]	1.44	2.24	22.4
7.47[b]	1.44	2.24	22.6
7.13[b]	1.44	2.98	30.4
7.48[b]	1.44	2.99	31.7
7.14[b]	1.44	3.72	34.9
7.14[a]	1.44	3.74	35.6
7.46[b]	1.44	4.49	42.5
7.46[b]	1.44	5.23	47.5
7.46[b]	1.44	5.98	54.8

a. Data from present study.

b. Data from Steinhaus and Lee[12].

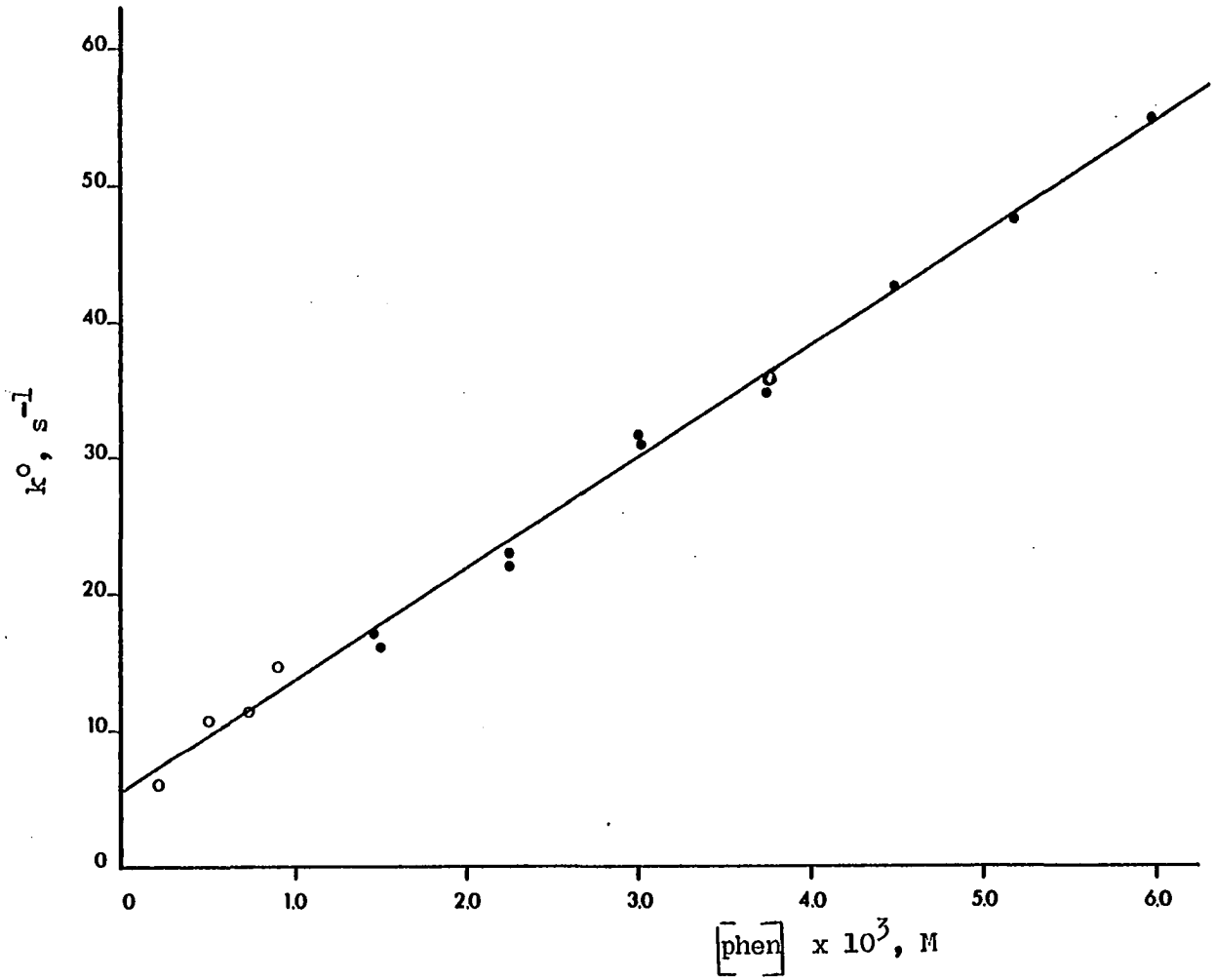

FIGURE 14. Dependence of k^o on [phen] for the $Ni(trien)^{2+}$ - phen Reaction; Points Marked o From This Study, • From Reference 12

to be linear over the entire concentration range of phen, which was varied by a factor of 28. A least-squares analysis of the data gave values for the slope and intercept which are k_{phen}^{NiT} and k_b respectively. These latter values are listed in Table 11.

Ni(trien)$^{2+}$ - Sarcosine Reaction

Studies on the reaction between Ni(trien)$^{2+}$ and sarcosine were monitored at 242 nm, over the pH range 6.9 to 8.8. The reaction was faster than the analogous NiEDDA-sarcosine reaction. In addition, problems associated with background noise showed up in percent transmittance values, and consequently, more scatter appeared in the values of measured rate constants.

Table 14 summarizes the kinetic data for the Ni(trien)$^{2+}$-sarcosine system. When plots were made of k^o against total sarcosine concentration $[sar]_T$, the scatter in the data prevented obtaining any reliable value of k_b, the intercept. In order to avoid the latter problem, the data were plotted as k^o vs. the concentration of sar^-, $[sar^-]$. A plot of k^o as a function of $[sar^-]$ is shown in Figure 15.

In order to deduce a value of the intercept of the curve shown in Figure 15, it was assumed that the observed curve could be described by the formula:

$$k^o = k_b + \frac{ab[sar^-]}{1 + a[sar^-]} \qquad (34)$$

This was thought to be a reasonable assumption, for the behavior shown in Figure 15 appears similar to that previously described for the reactions of NiEDDA with both gly and sar. Furthermore such

TABLE 14

Experimental Values of Rate Constants k^o for the $Ni(trien)^{2+}$-Sarcosine Reaction[a]

pH	$[Ni(trien)^{2+}] \times 10^3$ M	$[sar]_o \times 10^2$ M	$[sar^-] \times 10^4$ M	k^o[b] s^{-1}
6.90	1.48	4.00	0.325	19.2
7.20	1.90	2.20	0.355	18.3
7.19	1.56	2.00	0.376	19.0
6.89	1.90	6.00	0.478	19.1
7.20	1.90	4.00	0.648	20.2
6.89	1.83	10.0	0.802	20.5
7.18	1.56	4.00	0.932	20.9
7.18	1.38	8.0	1.24	21.4
7.19	1.90	7.95	1.27	22.2
7.19	1.90	10.0	1.58	20.8
7.18	1.56	10.0	1.55	20.9
7.50	1.49	5.00	1.62	23.7
7.50	1.49	8.00	2.58	23.3
7.50	1.49	10.0	3.22	25.1
7.89	1.19	3.50	3.34	27.4
7.90	1.19	5.50	4.42	30.1
7.89	1.19	8.00	7.60	40.4

TABLE 14 (continued)

8.31	1.19	5.00	10.2	37.1
8.32	1.19	6.00	12.4	43.8
8.61	1.19	3.50	14.1	40.8
8.61	1.19	4.50	18.0	49.7
8.61	1.19	5.50	21.8	51.1
8.63	1.19	6.52	27.5	55.2
8.82	1.19	5.00	31.7	59.3

a. Sar^- (N = methylglycinate ion) concentration calculated from distribution fraction curve

b. All runs: I = 0.1 M, T = 25.0 ± 0.1° C

behavior was reported for the analogous $Ni(trien)^{2+}$-gly reaction. When equation (34) is expanded, using the binomial theorem on the denominator, the resulting power series can be written in the form:

$$k^o = k_b + abx - ba^2x^2 + ba^3x^3 - ba^4x^4 + \ldots. \qquad (35)$$

In the above equation, the variable x represents the concentration of sar^-, $x = [sar^-]$. For low values of x, equation (35) reduces to

$$k^o = k_b + abx \qquad (36)$$

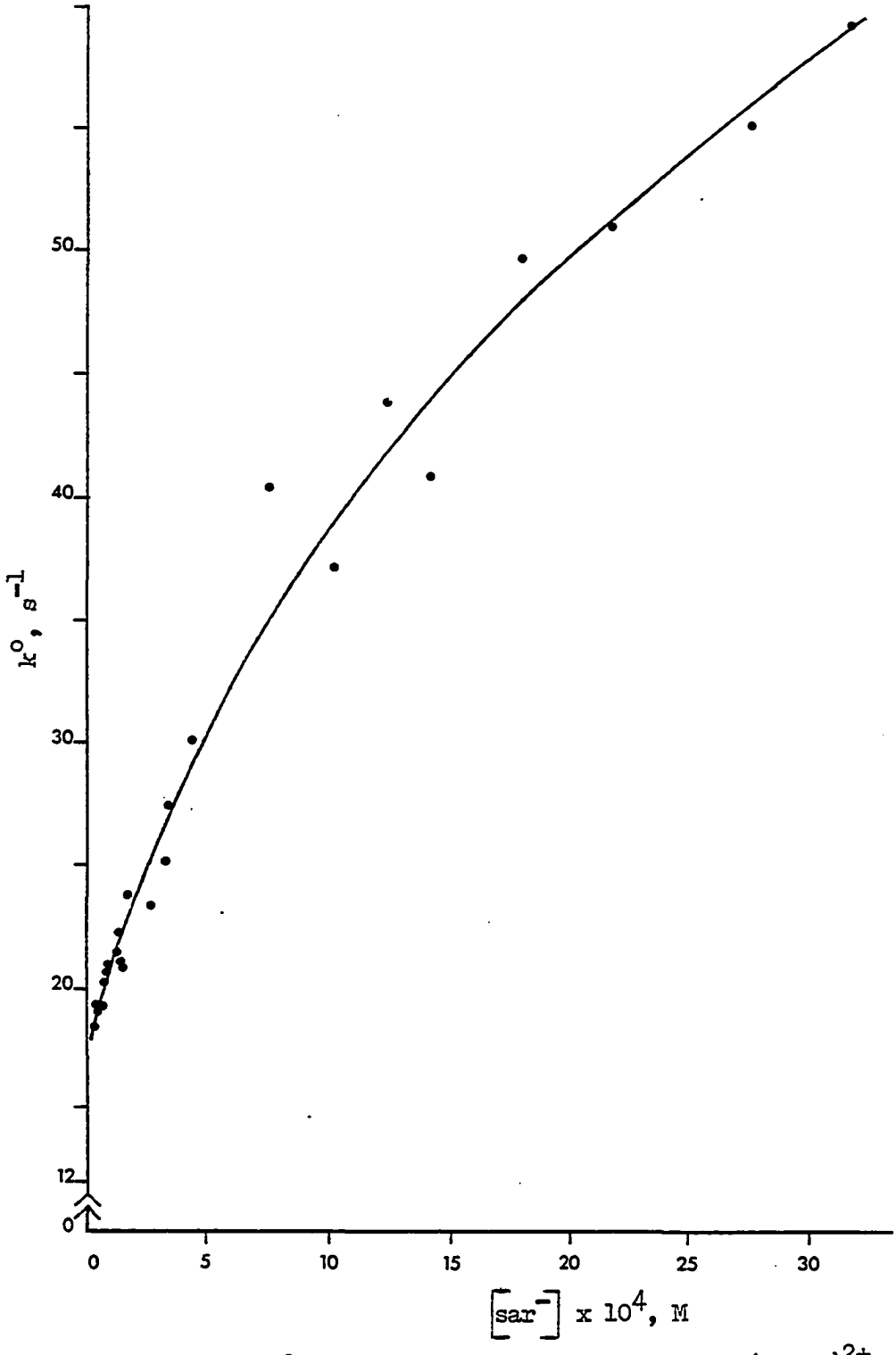

FIGURE 15. Plot of k^o vs. Sar Concentration for the $Ni(trien)^{2+}$ - sar Reaction

A least-squares analysis of the data in terms of equation (36), in the concentration range from 3.25×10^{-5} to 1.27×10^{-4} M, gave an intercept of 17.7 s^{-1}; the plot is shown in Figure 16.

A second method was used to verify that an intercept of 17.7 s^{-1} is a reasonable value. The second method involved a least-squares curve fit to the data plotted in Figure 16, using polynomials of various degrees. A computer program was used for the calculation of the polynomial coefficients for polynomials whose degree varied from 4 to 9. The intercepts obtained from the calculations are as follows:

polynomial degree	4	5	6	7	8	9
k_b, s^{-1}	17.40	17.94	17.80	17.81	17.51	17.76

These results indicate that an intercept of 17.7 s^{-1} is reasonable.

The intercept k_b was then subtracted from k^o of equation (35) to obtain the formula

$$k^{o\bullet} = k^o - k_b = \frac{ab[sar^-]}{1 + a[sar^-]} \qquad (37)$$

A plot of $k^{o\bullet}$ vs. $[sar^-]$ is shown in Figure 17. Equation (37) can be rearranged to linear form:

$$\frac{1}{k^{o\bullet}} = \frac{1}{ab[sar^-]} + \frac{1}{b} \qquad (38)$$

A least-squares fit of the data plotted according to equation (38)

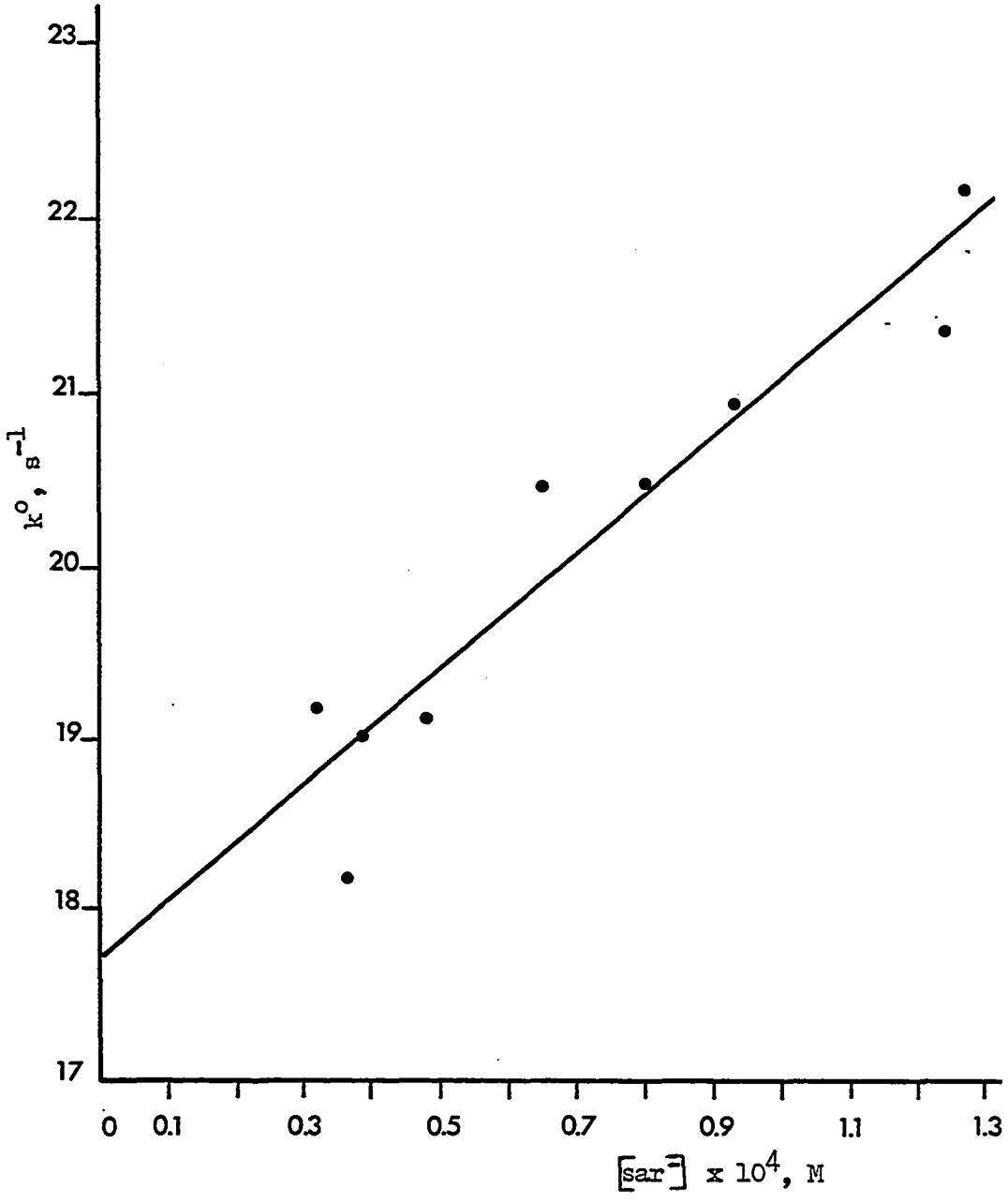

FIGURE 16. Resolution of Data to Obtain an Intercept for the $Ni(trien)^{2+}$ - sar Reaction

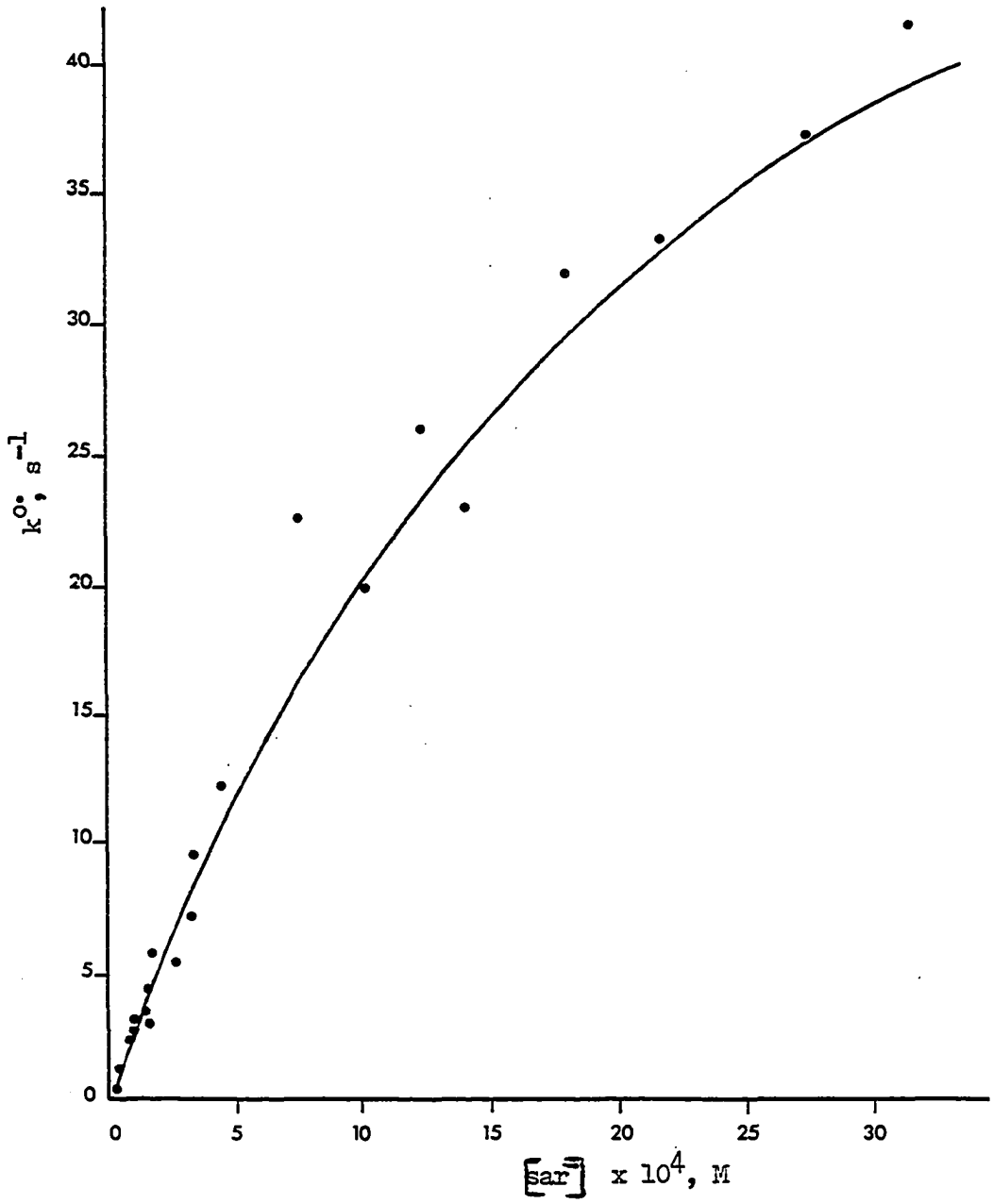

FIGURE 17. Plot of $k^{o\bullet}$ vs. Sar^- Concentration for the $Ni(trien)^{2+}$ - sar^- Reaction

is shown in Figure 18. This plot covers a $[sar^-]$ concentration range from 3.3×10^{-4} to 3.2×10^{-3} M. The resolved rate constants were calculated from the slope and intercept of the line shown in Figure 18. These values are given in Table 11.

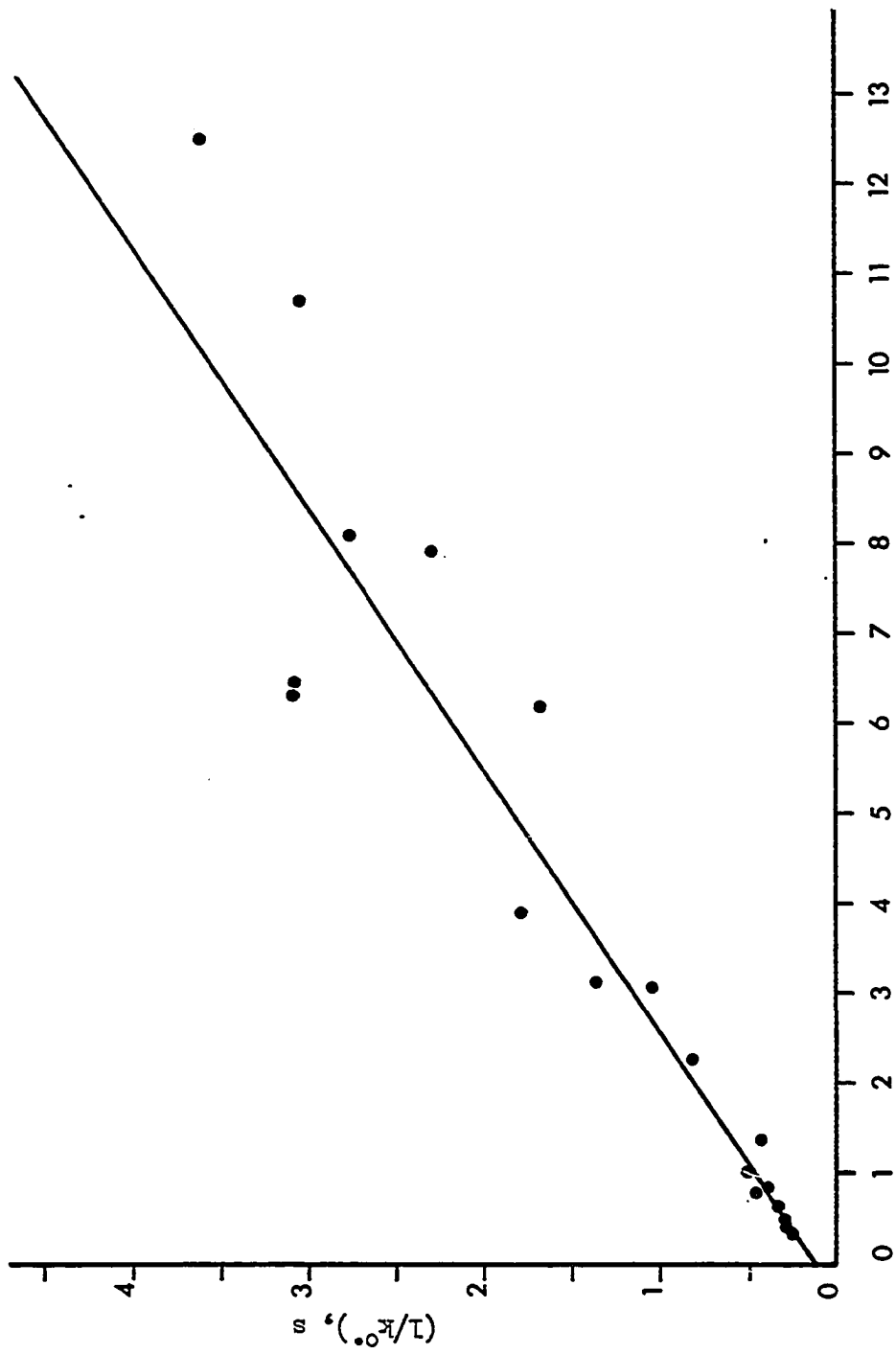

FIGURE 18. Resolution of k^{o} into a and b for the Ni(trien)$^{2+}$ - sar Reaction

CHAPTER IV

DISCUSSION

Predicted Rate Constants

As stated in the Introduction, the Eigen-Tamm equations (7) and (8) are useful in predicting formation rate constants only for idealized systems, for these equations are not corrected for the effects that the ligands L' and L_2 exert on the rate of formation involved in the reaction

$$NiL' + L_2 \longrightarrow L'NiL_2 \qquad (39)$$

In equation (39), L' corresponds to a multidentate ligand coordinated to the nickel (waters are omitted) while L_2 is an attacking bidentate ligand. Experimental evidence has been advanced to show that modifications of the Eigen-Tamm mechanism are necessary. Three of the most important factors that have better defined the nature of ternary complex formation reactions, and which may be relevant to the present study include:

(1) Stacking interactions

(2) ICB (internal conjugate base) effects

(3) Steric hindrance effects

Each of the above effects depends on the nature of both L' and L_2. In the systems under study, involving phen and bipy, stacking interactions can be ruled out because the coordinated species EDDA and

trien do not contain aromatic rings. The second factor mentioned above, the ICB effect, is precluded for phen, bipy, and enH^+, but must contribute to the reactions involving en, gly, and sar. This is because the two basic donor atoms in these latter ligands, whose second pK_a's are high enough (above 8), allow them to form hydrogen bonds with water molecules coordinated to the nickel ion. ICB effects will be discussed in more detail in later sections. The third effect presented above, the one involving steric hindrance, and its mechanistic consequences are the focal point of the present study, and will be discussed in detail in the following sections.

The mechanism proposed by Eigen and Tamm (Introduction, equations (1) to (3)), can be used to describe the addition of a bidentate ligand L_2^{n-} (of charge n-) to a tetradentate nickel(II) complex represented by $(L')Ni(H_2O)_2^{m+}$ (of charge m+). Following formation of an outer sphere complex A, the model involves formation of a singly attached intermediate B, as represented in equation (40).

$$\underset{A}{(L')Ni(H_2O)_2 \cdot L_2}^{m-n} \rightleftharpoons \underset{B}{(L')(H_2O)Ni\text{-}L\text{-}L}^{m-n} + H_2O \qquad (40)$$

Intermediate B is formed through the loss of water from the inner coordination sphere of the nickel (II) complex A. The forward rate constant for the process represented in Eq. (40) is denoted k^{Ni-H_2O}. As stated in the Introduction, equation (7) represents the second-order formation rate constant k_f for the Eigen-Tamm mechanism. In the derivation of equation (7) of the Introduction, it was assumed

that the outer-sphere reaction was rapid, that the steady-state approximation on B was valid, and that the reverse reaction of the final step could be neglected. In order to derive equation (8), a further assumption is necessary, that ring closure is much faster than the rate of water loss as represented above in equation (40). Using these four assumptions, k_f is predicted from calculated values of K_{os} and independently measured values of k^{Ni-H_2O}, as given in equation (41).

$$k_f = K_{os}\left(\frac{6-n}{6}\right) k^{Ni-H_2O} \qquad (41)$$

In the above equation, the factor (6-n)/6 is a statistical correction for the number of vacant coordination sites in the n-chelated nickel(II) complex relative to those available in aquonickel(II). The statistical factor is 2/6 when n = 4. Actually, equation (41) can be used when the rate constant for ring closure is nearly equal to the rate of water loss. In this case, $k_f = (1/2)K_{os}k^{Ni-H_2O}$ and the predicted rate constant falls within the experimental error of the measured rate constant.

When ICB effects are present and it is desired to eliminate them from a comparison of predicted and experimental results, equation (41) can not be used to predict k_f values. Another method for calculating k_f exists. Consider the addition of a bidentate ligand L_2^{n-} to the aquated nickel ion, $Ni(H_2O)_6^{2+}$, as given in equation (42).

$$Ni(H_2O)_6^{2+} + L_2^{n-} \rightleftharpoons (H_2O)_4Ni(L_2)^{2-n} + 2H_2O \qquad (42)$$

Let the observed rate constant for the above reaction be represented by $k^{L}_{Ni}(exp)$. The rate constant for water loss from $Ni(H_2O)_6^{2+}$ is k^{Ni-H_2O}. Now consider the formation reaction as given in equation (39). The rate constant for water loss from the complex NiL' is $k^{NiL'-H_2O}$. The formation rate constant for the reaction given in equation (39) can then be predicted by multiplying $k^{L}_{Ni}(exp)$ by a correction factor for the relative rates of $Ni-H_2O$ bond rupture for the complexes $Ni(H_2O)_2L'$ and $Ni(H_2O)_6^{2+}$ respectively. The result is given in equation (43).

$$k_f = \frac{k^{NiL'-H_2O}}{k^{Ni-H_2O}} \times \left(\frac{6-n}{6}\right) \times k^{L}_{Ni}(exp) \qquad (43)$$

In the above equation, (6-n)/6 is a statistical factor, as defined in equation (41).

When formation rate constants are predicted using equation (41), it is necessary to evaluate both K_{os} and k^{Ni-H_2O}. The association constant K_{os} for the outer-sphere complex is estimated from diffusion theory using statistical considerations. The proposed equation[14,15] for K_{os} is written:

$$K_{os} = \frac{4\pi Na^3}{3000} \exp(-U/kT) \qquad (44)$$

In the above formula:

(a) k is Boltzmann's constant

(b) T is temperature (K)

(c) N is Avogadro's number

(d) a represents the center to center distance between the ligand and Ni^{2+}

(e) U is the Debye-Huckel interionic potential, given by

$$U = \frac{Z_M Z_L e^2}{a^2 D (1 + ca)} \qquad (45)$$

In Eq. (45),

(f) Z_M and Z_L are the formal charges on each of the reacting species M and L (metal and ligand respectively)

(g) e represents the electronic charge

(h) D is the dielectric constant of solvent (D = 78.59 for H_2O)

(i) c is the Debye-Huckel ion atmosphere parameter

When one or both of the reacting species is uncharged, Eq. (44) reduces to:

$$K_{os} = \frac{4\pi N a^3}{3000} = 2.52 \times 10^{21} a^3 \qquad (46)$$

Equation (46) is applicable to the systems involving NiEDDA and the bidentate ligands enH^+, bipy, and phen. The same equation holds for the reaction of $Ni(trien)^{2+}$ with both bipy and phen. From molecular scale models, the value of a is found to be 4×10^{-8} cm. Substitution of this value into equation (46) yields $K_{os} = 0.16\ M^{-1}$ for each of the above systems.

When both of the reacting species are charged, Eq. (44) must be used to calculate K_{os}. In particular, for the $Ni(H_2O)_6^{2+}$-enH^+ reaction, Rorabacher[16] has reported a modified form of Eq. (44):

$$K_{os} = 2.52 \times 10^{21} a^3 \exp\left(\frac{-2e^2}{a'DkT}\right) \qquad (47)$$

In this equation, a' is the center to center distance between the metal ion and the protonated nitrogen on enH^+. Using $a' = 7.0 \times 10^{-8}$, and $a = 3.5 \times 10^{-8}$ cm in Eq. (47) gives $K_{os} = 0.014\ M^{-1}$.

According to equation (41), the formation rate constant k_f can be calculated using the above derived values of K_{os}. These values are given in Table 15. However, for the other reactant systems under study, equation (43) is used to predict k_f. The data used for this latter calculation, along with the predicted values of k_f are also given in Table 15. A summary of all of the predicted and measured rate constants for each of the systems under study is presented in Table 16.

Reactions of Diamines With NiEDDA and $Ni(trien)^{2+}$

NiEDDA-Phen Reaction

The experimental values of the formation rate constant k_f is lower than predicted by a factor of 2 (see Table 16). The difference is similar to that observed for the $Ni(H_2O)_6^{2+}$-phen reaction, and lies within the limits of reliability of the predicted rate constant. Thus in this case EDDA exerts no steric effect.

TABLE 15

Predicted Values of Formation Rate Constants

System	K_{os} M^{-1}	k^{Ni-H_2O} [a] s^{-1}	k_f $M^{-1}s^{-1}$
	Diamines		
NiEDDA-bipy	0.16	1.8×10^5	9.6×10^3
NiEDDA-phen	0.16	1.8×10^5	9.6×10^3
$NiEDDA-enH^+$	0.16	1.8×10^5	9.6×10^3
$Ni(trien)^{2+}$-bipy	0.16	5.0×10^6	2.7×10^5
$Ni(trien)^{2+}$-phen	0.16	5.0×10^6	2.7×10^5
$Ni(trien)^{2+}-enH^+$	0.014	5.0×10^6	2.3×10^4
NiEDDA-en	0.16	1.8×10^5	9.6×10^3

System	$k_{Ni}^{L'}$(expt.) $M^{-1}s^{-1}$	$k^{NiL'-H_2O}$ [a] s^{-1}	$\frac{k^{NiL'-H_2O}}{k^{Ni-H_2O}}$ [a]	k_f $M^{-1}s^{-1}$
	Amino Acids			
NiEDDA-gly	2.2×10^4	1.8×10^5	6.6	4.9×10^4
NiEDDA-sar	1.3×10^4	1.8×10^5	6.6	2.9×10^4
$Ni(trien)^{2+}$-sar	1.3×10^4	5.0×10^6	180	7.8×10^5

a. Reference 6

TABLE 16

Summary of Predicted and Experimental Rate Constants for the Reactions of Diamines and Amino Acids with $Ni(H_2O)_6^{2+}$(Ni), NiEDDA (NiE), and $Ni(trien)^{2+}$(NiT)

Part a

System	k_b s^{-1}	Diamines Predicted $k_f \times 10^{-3}$ $M^{-1}s^{-1}$	Experimental $k_f \times 10^{-3}$ $M^{-1}s^{-1}$	Ratio
Ni-bipy	-[a]	4.5[b]	1.6[c]	2.8
Ni-phen	-	4.5[b]	3.2[c]	1.4
NiE-bipy	8.0×10^{-2}	9.6	5.5	1.7
NiE-phen	3.0	9.6	4.3	2.2
$NiE\text{-}enH^+$	-	9.6	1.0	9.6
NiT-bipy	0.18	270	7.6	36
NiT-phen	5.3	270	8.2	33
$NiT\text{-}enH^+$	-	23	1.3	18
NiE-en	-	9.6	34	0.28

a. Data not given, reference 1

b. Predicted using equation (41), rate of water loss values, $k^{Ni\text{-}H_2O} = 2.8 \times 10^4\ s^{-1}$ from reference 1

c. Data from reference 1

TABLE 16 - Part b

Amino Acids

System	k_b s^{-1}	k_1 M^{-1}	k_2 s^{-1}	Experimental $k_f \times 10^{-3}$ $M^{-1}s^{-1}$	Predicted $k_f \times 10^{-3}$ $M^{-1}s^{-1}$	Ratio
Ni-gly	-	-	-	22[b]	-	-
Ni-sar	-	-	-	13[b]	-	-
NiE-gly	0.45	190	44	8.4	49	5.8
NiE-sar	0.41	93	44	4.1	22	5.4
NiT-gly[c]	8.7	690	130	90	1.3×10^3	14
NiT-sar	17.7	430	68	29	7.8×10^2	27

a. Indicates no data available or not needed for the purpose of this study

b. Ref. 17

c. Ref. 12

Ni(trien)$^{2+}$-Phen Reaction

For the Ni(trien)$^{2+}$-phen system, the ratio of the predicted rate constant to the experimental value, as shown in Table 16, is 33. This sharp reduction in the value of k_f appears to be due to a steric hindrance of trien. However, whether the effect involves blocking by trien at the initial point of coordination or hindrance during ring closure can not be discerned.

NiEDDA-Bipy Reaction

For the addition of bipy to NiEDDA, the measured value of k_f (Table 16) is lower than predicted by only a factor of 1.7. This difference is almost identical with that found in the NiEDDA-phen system, and is too small to be significant. Thus there is no steric effect due to EDDA.

$Ni(trien)^{2+}$-Bipy Reaction

For the $Ni(trien)^{2+}$-bipy reaction (Table 16), the ratio of k_f values (predicted vs. experimental) is 36. This result shows that, as with the $Ni(trien)^{2+}$-phen system, trien contributes a steric component to the formation rate constant. The presence of a steric effect seen when trien is coordinated to nickel probably is due to the two protons attached to the terminal nitrogens as well as the protons on the carbons that are in a position alpha to the terminal nitrogens. The lack of a steric effect due to coordinated EDDA must be attributed to the unclutered nature of the acetate dentate site having only an unsubstituted atom, oxygen, involved in the bond to the nuclei. This is readily seen by observing molecular models.

NiEDDA-enH^+ vs. $Ni(trien)^{2+}$-enH^+

The formation rate constants for the reactions of enH^+ with either nickel complex are lower than expected, as shown in Table 16. In each case the extra proton appears to block the reaction. Also the tetrahedral nitrogen of enH^+, when compared with the planar

nitrogens of phen and bipy, may cause steric hindrance, which is greater for trien. There is also a statistical effect since enH^+ is a monodentate ligand. Equation (47) does not take into account a statistical component to the reaction rate, due to an attacking ligand.

It has been reported[18] that protonation of a reactive species such as en, can cause a pronounced decrease in the rate of formation of a binary complex. A comparison of the formation rate constant of en with that of enH^+ shows this effect for NiEDDA. An ICB effect enhances the rate of the reaction involving en; enH^+ can not show an ICB effect.

Stability Constants for the Diamine Complexes of NiEDDA and $Ni(trien)^{2+}$

The stability constants K_s for the addition of either phen or bipy to either NiEDDA or $Ni(trien)^{2+}$ are given in Table 17. These values were calculated from the measured ratio of rate constants k_f to k_b. Also listed in Table 17, are stability constants for the formation of $Ni(phen)^{2+}$ and $Ni(bipy)^{2+}$. A comparison of the K_s values between the respective binary and ternary complexes of phen with the series of nickel(II) complexes: $Ni(H_2O)_6^{2+}$, NiEDDA, and $Ni(trien)^{2+}$, shows an enormous drop in stability for the latter two complexes relative to the former. This decrease in stability is attributed to a steric effect placed upon the fully coordinated ternary complex as a result of coordinated trien or EDDA. A comparison of the stability constants between the corresponding binary and ternary complexes containing bipy shows a much smaller effect.

TABLE 17

Stability Constants K_s for the Addition of Diamines and Amino Acids to $Ni(H_2O)_6^{2+}$, NiEDDA, and $Ni(trien)^{2+}$

Ligand	Stability Constant[a] (M^{-1}) $Ni(H_2O)_6^{2+}$	NiEDDA	$Ni(trien)^{2+}$
Phen	4.0×10^8[b]	1.4×10^3	1.6×10^3
Bipy	1.4×10^7[b]	6.9×10^4	4.2×10^4
Gly	6.0×10^5[c]	1.9×10^4	1.1×10^4[d]
Sar	3.2×10^5[c]	1.0×10^4	1.6×10^3

a. $T = 25^{\circ}C$, ionic strength = 0.1 M

b. Reference 19

c. Reference 20

d. Reference 12

Evidently the coordinated ligands trien and EDDA exert a small effect on the stability of the ternary complexes containing bipy to phen. One possible reason is that a degree of twisting or flexibility is required to chelate bipy or phen in the presence of EDDA or trien. Bipy has the flexibility but phen does not. A steric factor is not

present in the formation reactions of bidentate ligands with NiEDDA. Thus the large drop in stability seen when EDDA is coordinated to nickel must mean that the bonds formed with the bidentate ligand are considerably weaker thus increasing the dissociation rate. This may be due to a twisting of the bulky rings of phen and bipy.

Mechanism for the Reactions of the Diamines with NiEDDA and $Ni(trien)^{2+}$

For the reactions of either bipy or phen with NiEDDA, the measured formation rate constants are not significantly lower than the predicted values. Thus the reactions of the aromatic diamines appear to proceed at a normal rate and appear to obey equation (41). The Eigen-Tamm mechanism is used to describe the rate behavior, with formation of the singly bonded intermediate being the rate controlling step, as represented in equation (40).

The formation rate constants determined for the reactions of phen and bipy with $Ni(trien)^{2+}$ are lower than predicted by factors of 33 and 36 respectively. It is not known whether this effect is due to a steric hindrance at the initial point of coordination or to a sluggish ring closing step. Ring closure has been invoked[21] as partly limiting the formation rate of $Ni(bipy)^{2+}$. However, since in the present study, first-order behavior with respect to ligand concentration is always observed, it can be deduced from the experimental results that the steady-state approximation for the singly bonded intermediate appears valid, and also that the Eigen-Tamm reaction sequence appears valid. The Eigen-Tamm mechanism also

appears to represent the experimental behavior for the reactions of en or enH^+ with either NiEDDA or $Ni(trien)^{2+}$, since first-order behavior with respect to the concentration of ligand is observed.

Kinetic data for the addition of either phen or bipy to a series of nickel(II) complexes are shown in Table 18. A pronounced trend is shown by the four nickel(II) complexes whose k_f values increase in the order $Ni(H_2O)_6^{2+} <$ NiEDDA $<$ $Ni(trien)^{2+} <$ $Ni(tren)^{2+}$. This trend in k_f values parallels the trend shown by the rates of water loss, given by k^{Ni-H_2O} (column 3 of Table 18). However the relative increase of k_f values is not equal to the relative increase in k^{Ni-H_2O} values. Hence, a second factor is influencing the k_f values, lowering them below what is expected on the basis of ratios of water loss. This latter factor is steric hindrance. The last column in the bottom part of Table 18 shows the expected increase in k_f values as a result of rate of water loss. The two columns preceeding it show the actual increase observed relative to hexaaquo nickel, corrected for a statistical factor. It is very obvious that EDDA shows virtually no steric factor at all, but that trien and tren considerably hinder the formation reactions.

Reactions of Amino Acids With NiEDDA and $Ni(trien)^{2+}$

Mechanism

The kinetic results are similar for either glycine or sarcosine reacting with either nickel complex. As the concentration of L^- (either gly^- or sar^-) is systematically increased, the linear sections of the k^o vs. $[L^-]$ plots bend and then appear to reach a

TABLE 18

Formation Rate Constants and Experimental Values of Ratios of Water Loss for the Addition of Phen and Bipy to a Series of Nickel(II) Complexes

Complex	Formation Rate Constants and Rate of Water Loss k_f(phen) $M^{-1}s^{-1}$	k_f(bipy) $M^{-1}s^{-1}$	k^{Ni-H_2O}[a] s^{-1}
$Ni(H_2O)_6^{2+}$	4.1×10^3[b]	2.0×10^3[b]	2.7×10^4
NiEDDA	4.3×10^3	5.5×10^3	1.8×10^5
$Ni(trien)^{2+}$	8.2×10^3	7.6×10^3	5.0×10^6
$Ni(tren)^{2+}$	1.3×10^4[c]	1.0×10^4[c]	9.0×10^6

Complex	Experimental Ratio phen $\frac{k_L^{NiL}}{k_L^{Ni(H_2O)_6}} \times 3$	bipy $\frac{k_L^{NiL}}{k_L^{Ni(H_2O)_6}} \times 3$	Ratio of Water Loss $\frac{k^{NiL-H_2O}}{k^{Ni(H_2O)_6-H_2O}}$
EDDA	3.0	8.3	6.7
trien	6.0	11.4	180
tren	9.5	15.0	330

a. Reference 6

b. Reference 17

c. Reference 10

plateau at high concentrations. This latter behavior was illustrated in Figures 7, 10, and 15 for the respective reactions studied. Furthermore, such a dependence of $k^{o\bullet}$ versus $[L^-]$ was recently reported for the $Ni(trien)^{2+}$-gly-reaction[12]. The observed behavior indicates a shift in reaction order from first to zero as the concentration of L^- is increased. The empirical equation describing the $k^{o\bullet}$ versus $[L^-]$ plots, is shown in equation (48).

$$k^{o\bullet} = \frac{ab[L^-]}{(1 + a[L^-])} \qquad (48)$$

At low concentrations of L^-, the second term in the denominator of equation (48) is negligible, and an expression of the first-order with respect to $[L^-]$ is obtained (equation 49).

$$k^{o\bullet} = ab\,[L^-] \qquad (49)$$

In contrast, at high $[L^-]$, equation (48) simplifies to an expression that is zero-order with respect to $[L^-]$.

$$k^{o\bullet} = b \qquad (50)$$

In order to deduce a mechanism consistent with the above results, it is helpful to consider the following sequence of reactions:

$$(H_2O)_2NiL'_4 + NHRCH_2COO^- \overset{K_{os}}{\rightleftharpoons} \underset{A}{(H_2O)_2Ni(L'_4)\cdot(NHRCH_2COO^-)} \qquad (51)$$

$$A \underset{k_{-1}}{\overset{k_1}{\rightleftharpoons}} \underset{B}{(H_2O)(L'_4)Ni\text{-}O\text{-}CH_2NHR} + H_2O \qquad (52)$$

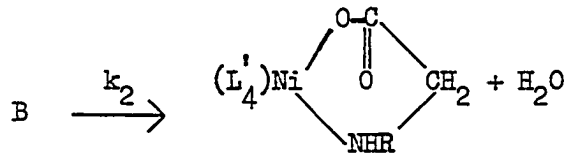

(53)

C

In the above mechanism, L'_4 represents the tetradentate ligand, either EDDA or trien, coordinated to nickel. The nickel complex has no charge when the coordinated ligand is EDDA, but has a +2 charge when trien is coordinated. The various intermediates shown in the above mechanism are analogous to those described in the Eigen-Tamm mechanism, but the same assumptions do not apply. In the above mechanism, $NHRCH_2COO^-$ represents either gly^- (R = H) or sar^- ($R = CH_3$). The initial bonding of the amino acid through the carboxyl group (first step) is well established[1,22]. The remaining steps in the above mechanism are as previously defined. In order to derive a rate law of the form of the empirical equation (48), the second step of the above mechanism is written as an equilibrium, instead of using the steady state approximation to describe species B. Both steps (51) and (52) are assumed to represent rapid equilibria with step (53) being rate controlling, i.e., $k_{-1} \gg k_2$.

The above mechanism can be written in simplified form as a two step process:

$$(H_2O)_2NiL'_4 + NHRCH_2COO^- \underset{}{\overset{K_1}{\rightleftharpoons}} B + H_2O \qquad (54)$$

$$B \xrightarrow{k_2} C + H_2O \qquad (55)$$

In this simplified mechanism the equilibrium constant K_1 is defined as

$$K_1 = K_{os}\frac{k_1}{k_{-1}} \tag{56}$$

The total concentration of the tetradentate complex $(H_2O)_2NiL'_4$ is written

$$\left[NiL'_4\right]_T = \left[NiL'_4\right] + \left[B\right] \tag{57}$$

Under pseudo-first-order conditions, the concentration of gly o sar is in excess. The rate of decrease of total NiL'_4 concentration becomes

$$\frac{-d\left[NiL'_4\right]}{dt} = k^{o\bullet}\left[NiL'_4\right]_T = k_2\left[B\right] \tag{58}$$

The equilibrium constant K_1, describing the formation of species B, is written

$$K_1 = \frac{\left[B\right]}{\left[NiL'_4\right]\left[L^-\right]} \tag{59}$$

Substituting equations (57) and (59) into Eq. (58), and rearranging gives Eq. (60)

$$k^{o\bullet} = \frac{k_2K_1\left[L^-\right]}{(1 + K_1\left[L^-\right])} \tag{60}$$

This latter equation corresponds to equation (48) with $K_1 = a$, and $k_2 = b$. At low $\left[L^-\right]$ the second-order rate constant describing formation of ternary complex is

$$k_f = \frac{k^{o\bullet}}{[L^-]} = k_2K_1 \qquad (61)$$

From equation (60), at low L^-, $k^{o\bullet} = k_2K_1[L^-]$ so that first-order rate behavior with respect to L^- is observed. On the other hand, at high $[L^-]$, $k^{o\bullet} = k_2$ and the reaction being studied is ring closure which is rate determining. In terms of a modified Eigen-Tamm model, for this latter condition to hold, $k_{-1} \gg k_2$. Table 16 lists values for the ring closure rate constants whose values lie in the range 44 to 130 s^{-1}. Although no values have been directly measured for the dissociation rate constant k_{-1}, it can be approximated by the known value[23] for pentaaquonickel acetate: $k_{-1} = 5 \times 10^3\ s^{-1}$. Thus $k_{-1} \gg k_2$ and ring closing is rate limiting. The first two steps of the modified Eigen-Tamm mechanism, as stated before, can be combined to give equation (54) whose equilibrium constant is given by K_1. Table 16 lists values of K_1, which for the above systems, lie in the range 93 to 690 M^{-1}. Thus the equilibria leads to a buildup in concentration of the monocoordinated species B, so that the steady state approximation is no longer valid.

The foregoing discussion is consistent with an equilibrium-type mechanism for chelate formation. The first step of the mechanistic sequence must involve a rapid buildup of species B, accelerated by the increase in rate of water loss from coordinated trien or EDDA, coupled with a rapid dissociation of B to reactants, due to the first nickel-oxygen bond being weak. The second step involves a

slower removal of B during ring closure. This latter process is sterically hindered by either trien or EDDA.

Finally, the above equilibrium-type mechanism is in agreement with published results[22] showing that in equation (52), initial attack must come from the weakly basic carboxylate segment of the amino acid.

Predicted vs. Experimental k_f Values

NiEDDA

The second-order rate constant, denoted k_f, can be predicted using Eq. (43) and directly compared to the measured values as deduced from Eq. (60). Table 16 lists both the predicted and experimentally calculated values of k_f. For the formation of NiEDDA(gly)$^-$ and NiEDDA(sar)$^-$, the measured k_f values are lower than expected, but only by factors of 5.8 and 5.4 respectively. Moreover, the ring closure rate constant is about the same for each system. These results imply that the N-methyl group of sarcosine does not exert a large steric effect on either ring closure or on the overall rate of reaction. However, K_1(gly) is about two times larger than K_1(sar), indicating that the equilibrium leading to species B is somehow more hindered for the case of sar. This latter effect may be partly explained by consideration of the ICB effect. Both gly and sar have pK_a values about 8 and would proceed through an ICB mechanism. However, in comparison to gly, sar contains an N-methyl group, and therefore half as many protons are available

for hydrogen bonding. Hence the coordination of sar may be sluggish compared to gly, due to both a steric and statistical effect.

The fact that the experimental k_f values are just slightly lower than predicted ones masks the steric effect of EDDA. True Eigen-Tamm behavior follows the equation

$$k_f = \frac{K_{os}\, k_1\, k_2}{k_{-1} + k_2} \qquad (62)$$

But the reactions of NiEDDA with gly and sar follow the equation

$$k_f = \frac{K_{os}\, k_1 k_2}{k_{-1}} \quad \text{at low } [L^-] \qquad (63)$$

This latter equation is derived from the preceeding one by taking $k_{-1} >> k_2$. Coordinated EDDA greatly lowers k_2 while at the same time increasing k_1 and k_{-1}. Thus Eq. (62) reverts to Eq. (63) and a shift in mechanism occurs from steady state to equilibrium. However, the two effects, an increase in k_1 and k_{-1}, and a decrease in k_2 tend to somewhat offset each other so that the experimental k_f value is only a factor of about five lower than predicted. Thus, EDDA does exert a large effect which is seen through the mechanistic change and not through a comparison of k_f values.

Ni(trien)$^{2+}$

The resolved kinetic data for the reactions of Ni(trien)$^{2+}$ with gly and sar are presented in Table 16. The ratio of predicted to measured k_f values are 15 and 27 for gly$^-$ and sar$^-$ respectively.

The large difference again implies that trien exerts a larger steric effect than EDDA. The lower value of K_1 for sar relative to gly again shows steric hindrance of the methyl group in the ICB mechanism. Although ring closure rate constants are similar in the NiEDDA system, k_2 is much smaller for sar than for gly in the $Ni(trien)^{2+}$ system. This result shows that with trien, which has already been shown to exert a larger steric effect than EDDA, the N-methyl group does add further hindrance. Again, as with NiEDDA, the actual effect of trien on the formation can be appreciated by noting the mechanistic change rather than the comparisons of k_f values.

Stability Constants for Ternary Complexes Involving Gly and Sar

The stability constants K_s for the addition of gly^- and sar^- to $Ni(H_2O)_6^{2+}$, NiEDDA, and $Ni(trien)^{2+}$ are listed in Table 17. K_s is again calculated from the measured ratio of k_f to k_b. The stability of the complexes decrease in the order, $Ni(H_2O)_6L^+ <$ $NiEDDA(L)^- < Ni(trien)L^+$, where L^- is either gly^- or sar^-. Thus $Ni(trien)^{2+}$ shows the greatest steric effect. This observed decrease in the stability for ternary complexes containing amino acids is not nearly as great as observed for the corresponding K_s values shown in Table 17 for the complexes of phen and bipy with NiEDDA and $Ni(trien)^{2+}$. The stability constants for these latter complexes, especially those containing phen, are markedly lower.

ICB Effects of Gly and Sar

For the mechanism provided in equations (51) to (53), an ICB effect is involved in step (52). For this latter process the equilibrium constant has been given in equation (63). However, since equation (63) does not incorporate a term for an ICB effect, it can not be used to predict K_1. For the reactions of NiEDDA with either gly or sar, the ICB effect involves hydrogen bonding of an amine nitrogen to a coordinated water molecule. In order to estimate an ICB effect, it is helpful to consider the coordination of OAc to Ni^{2+} in water. Like the amino acids, OAc binds to aquated Ni^{2+} using a carboxyl group, but being monodentate, it can not have an ICB effect. Therefore, an estimate of the ICB effect in the reactions of gly or sar with NiEDDA can be made by taking the ratio of stability constants, K_1 to $K_1(OAc)$. The measured stability constant of $Ni(OAc)^+$ is 5.0 M^{-1}. The experimental values of K_1 (Table 16) for gly and sar reacting with NiEDDA are 190 and 93 M^{-1} respectively. Thus the ICB effects for the latter reactions are 39 (gly) and 19 (sar).

By using the above method, it is possible to obtain an estimate for the ICB effect involved in the reaction of sar with $Ni(trien)^{2+}$. However, because there are two possible ways for amino acids to hydrogen bond to this complex, the value of the ICB effect can not be assigned to a given type of hydrogen bonding. For example, hydrogen bonding can take place between the amine group of the amino acid and either a coordinated H_2O molecule on $Ni(trien)^{2+}$ or to one

of the protons on either end of trien. An ICB effect involving the end hydrogens of trien may lead to higher stability constants because the Ni-N bond is stronger than the Ni-O bond. This latter effect could lead to a stronger outer-sphere complex, and subsequently a higher rate of water exchange from an adjacent site on Ni, before the free N donor on sar can form an inner-sphere complex during ring closure. The calculated ICB effect for the sar-Ni(trien)$^{2+}$ reaction is then found to be 85, and this value represents an upper limit for the ICB effect. The corresponding upper limit for the reaction of gly with Ni(trien)$^{2+}$ has been reported[12] as 140.

Conclusions

The present study on ternary complex formation has found that a shift in the rate limiting step (from initial coordination to ring closure) can be brought about by a combination of two major effects that are related to the nature of the ligands involved. The first effect involves the steric hindrance exerted by a tetradentate ligand (EDDA or trien) already bound to nickel(II). The second influence involves the type of donor sites on the attacking bidentate ligand. For the reactions of bipy and phen, whose nitrogen donors are weakly basic, the Eigen-Tamm mechanism describes the kinetics. The same mechanism is deduced for the reactions of enH^{+}, which has only one readily available strong donor for initial bond formation. In contrast, the amino acids gly and sar, which have one strong and one weak donor, react with EDDA and Ni(trien)$^{2+}$ by an equilibrium-type mechanism whose rate controlling step involves ring closure.

Kinetically, for the Eigen-Tamm mechanism, the formula for the second-order rate constant is:

$$k_f = \frac{K_{os} k_1 k_2}{k_{-1} + k_2} \qquad (64)$$

In contrast, for the equilibrium-type mechanism, the formation rate constant is given by:

$$k^o = \frac{k_2 K_1}{1 + K_1[L^-]} + k_b \qquad (65)$$

where,

$$K_1 = K_{os} \frac{k_1}{k_{-1}} \qquad (66)$$

Suggestions For Further Study

Using NiEDDA and $Ni(trien)^{2+}$, it would be interesting to further study the effects that bidentate ligands exert on substitution reactions. One interesting study could involve the steric effects that N-alkyl groups exert. Thus one potential project could involve the reactions of N-ethylglycine and N,N-dimethylglycine. Another study could involve compounds with alkyl groups - substituted ethylenediamine. However, it would be even more interesting to study the reactions of 2-aminomethylpyridine and pyridine-2-carboxylic acid, for the combinations of donors in these bidentate ligands are different than those reported here, and should have interesting effects. From a large number of studies, it may be

possible to quantify the effects exerted in ternary complex formation reactions, and thereby arrive at an equation that is useful in predicting formation rate constants.

REFERENCES

1. Margerum, D. W., Cayley, G. R., Weatherburn, D. C., & Pagenkopf, G. K. Kinetics and mechanisms of complex formation and ligand exchange. In A. E. Martell (Ed.), Coordination chemistry (Vol. 2). Washington, D. C.: American Chemical Society, 1978.

2. Caldin, E. F. Fast reactions in solution. New York: John Wiley & Sons, 1964.

3. Eigen, M., & Tamm, K. Sound absorption in electrolytes as a consequence of chemical relaxation. I. Relaxation theory of stepwise dissociation. Z. Electrochem., 1962, 66, 93-107.

4. Martin, R. P., & Scharff, J. P. Mixed ligand complexes and their biological significance. In D. R. Williams (Ed.), Introduction to bio-inorganic chemistry. Springfield: Thomas, 1976.

5. Sigel, H. (Ed.). Metal ions in biological systems (Vol. 2). New York: Marcel Dekker, 1973.

6. Hunt, J. P. Water-exchange kinetics in labile aquo and substituted aquo transition metal ions by means of ^{17}O N M R Studies. Coord. Chem. Rev., 1971, 71, 1-10.

7. Jones, J. P., Billo, E. J., & Margerum, D. W. The effect of coordinated ligands on the rate of replacement of bound water by ammonia in nickel(II) complexes. II. J. Am. Chem. Soc., 1970, 92, 1875-1880.

8. Hague, D. W., & Kinley, K. Kinetics of ternary complex formation between nickel species and 5-nitrosalicylic acid. J. Chem. Soc., Faraday Trans., 1974, 249-253.

9. Cobb, M. A., & Hague, D. N. Kinetics of ternary complex formation between nickel(II) species and pyridine-2-azo-p-dimethylaniline. J. Chem. Soc., 1972, 68, 932-938.

10. Wilkins, R. G. Mechanisms of ligand replacement in octahedreal nickel(II) complexes. Acc. Chem. Res., 1970, 3, 408-416.

11. Farrar, D. T., Stuehr, J. E., Moradi-Araghi, A., Urbach, F. L., & Campbell, T. G. Ternary complex formation between a tetradentate nickel(II) chelate and additional donors. A kinetic and thermodynamic study. Inorg. Chem., 1973, 12, 1847-1851.

12. Steinhaus, R. K., & Lee, B. I. Ternary complex formation kinetics involving (triethylenetetramine)nickel(II) and bidentate ligands. Inorg. Chem., 1982, 21, 1829-1833.

13. Lee, B. I. Kinetic study of the formation of mixed ligand complexes formed from triethylenetetramine nickel(II) and bidentate ligands (Masters thesis, Western Michigan University, 1979). Masters Abstracts, 1980, 18, 314242.

14. Fuoss, R. M. Ionic association. III. The equilibrium between ion pairs and free ions. J. Am. Chem. Soc., 1958, 80, 5059-5061.

15. Eigen, M. Kinetics of high-speed ion reactions in aqueous solutions. Z. Phys. Chem. (Frankfurt am Main). 1954, N F 1, 176-200.

16. Rorabacher, D. B., Turan, T. S., Defever, J. A., & Nickels, W. G. Steric effects in chelation kinetics. The formation and dissociation of nickel(II) complexes with branched poly-(amino alcohols) related to ethylenediaminetetraacetic acid. Inorg. Chem., 1969, 8, 1498-1506.

17. Kustin, K., & Swinehart, J. Fast metal complex reactions. In S. J. Lippard (Ed.), Progress in inorganic chemistry (Vol. 13). New York: Interscience Publishers, 1970.

18. Taylor, R. W., Stepien, H. K., & Rorabacher, D. B. Kinetics of aquonickel(II) ion reacting with ethylenediamine. Evidence of the internal conjugate base effect and intramolecular hydrogen bonding. Inorg. Chem., 1974, 13, 1282-1289.

19. Smith, R. M., & Martell, A. E. Critical stability constants, amines (Vol. 2). New York: Plenum Press. 1975.

20. Smith, R. M., & Martell, A. E. Critical stability constants, amino acids (Vol. 1). New York: Plenum Press, 1975.

21. Diebler, H. Equilibrium and kinetics of the formation of monobipyridyl complexes of chromium(II) and copper(II). Ber. Bunsenges Phys. Chem., 1970, 74, 268-276.

22. Lin, C., & Rorabacher, D. B. Electrostatic effects in coordination kinetics. Reaction of nickel(II) ion with a cationic unidentate ligand as a function of solvent dielectric. Inorg. Chem., 1973, 12, 2402-2410.

23. Hoffman, H. Kinetics of dissociation and formation of nickel chelate complexes of different bidentate ligands (hydroxycarboxylates, aminocarboxylates, dicarboxylates). Ber. Bunsenges Phys. Chem., 1969, 73, 432-437.

24. Sillen, L. & Martell, A. E. Stability constants of metal ion complexes. London: The Chemical Society, 1964.